

SELF-SIMILAR COLLISIONLESS SHOCKS

BOAZ KATZ¹, URI KESHET² AND ELI WAXMAN¹*Draft version February 7, 2020*

ABSTRACT

Observations of γ -ray burst afterglows suggest that the correlation length of magnetic field fluctuations in the downstream of relativistic non-magnetized collisionless shocks grows with the distance from the shock to scales much larger than the plasma skin depth. We argue that this indicates that the plasma properties are described by a self-similar solution, and derive constraints on the scaling properties of the solution. For example, we find that the scaling of the characteristic magnetic field amplitude with distance from the shock is $B \propto D^{s_B}$ with $-1 < s_B \leq 0$, that the spectrum of accelerated particles is $dn/dE \propto E^{-2/(s_B+1)}$, and that the scaling of the magnetic correlation function is $\langle B_i(\mathbf{x})B_j(\mathbf{x}+\Delta\mathbf{x}) \rangle \propto \Delta\mathbf{x}^{2s_B}$ (for $\Delta x \gg D$). We show that the plasma may be approximately described as a combination of two self-similar components: a kinetic component of energetic particles, and an MHD-like component representing "thermal" particles. We argue that the thermal component may be considered as an infinitely conducting fluid, in which case $s_B = 0$ and the scalings are completely determined (e.g. $dn/dE \propto E^{-2}$ and $B \propto D^0$, with possible logarithmic corrections). Similar claims can be made regarding non-relativistic shocks such as in supernova remnants, if the upstream magnetic field can be neglected. If self-similarity holds, it has important implications for any model of particle acceleration and/or field generation. For example, we show that the velocity-angle diffusion coefficient in diffusive shock acceleration models must satisfy $D_{\mu\mu}(\mathbf{p}, D) = D^{-1}\tilde{D}_{\mu\mu}(\mathbf{p}/D)$ (where \mathbf{p} is the particle momentum), and that a previously suggested model for the generation of a large scale magnetic field through hierarchical merger of current-filaments should be generalized. The generalization leads to qualitative changes in the model's major predictions, e.g. a constant merger velocity is predicted rather than increasing velocity approaching the speed of light. Finally, we point out that the self-similarity assumptions may be tested through the implied evolution of homogenous (time-dependent) plasmas, which may be accessible to direct numerical simulations: We predict that the inclusion (at the initial conditions) of a power-law spectrum of high energy particles, $dn/dE \propto E^{2+l_p}$, would lead to magnetic field evolution following $B \propto t^{-(l_p+4)/2(l_p+3)}$.

Subject headings: acceleration of particles — shock waves — gamma rays: bursts — magnetic fields — plasmas — supernova remnants

1. INTRODUCTION

Due to the low densities characteristic of a wide range of astrophysical environments, shocks observed in many astrophysical systems are collisionless, i.e. mediated by collective plasma instabilities rather than by particle-particle collisions. For example, collisionless shocks play an important role in supernova remnants (e.g. Blandford & Eichler 1987), jets of radio galaxies (e.g. Begelman et al. 1994; Maraschi 2003), gamma-ray bursts (GRB's, e.g. Zhang & Mészáros 2004), and the formation of the large scale structure of the Universe (e.g. Loeb & Waxman 2000). Although collisionless shocks have been studied for several decades, theoretically and experimentally, in space and in the laboratory, a self-consistent theory of collisionless shocks based on first principles has not yet emerged (see, e.g., comments in Krall 1997).

Observations of GRB "afterglows," the delayed low energy emission following the prompt γ -ray emission, provide a unique probe of the physics of collisionless shocks. Current understanding suggests that the afterglow radiation observed is the synchrotron emission of energetic, non-thermal electrons in the downstream of a strong collisionless shock driven into the surrounding interstellar medium (ISM) or stellar wind. These collisionless shocks start out highly relativistic, with shock Lorentz factor $\gamma_s \sim 100$ on time scale of min-

utes after the GRB, and gradually decelerate to $\gamma_s \sim 10$ on a day time scale and $\gamma_s \sim 1$ on a month time scale. This allows one to probe the physics of the shocks over a wide range of Lorentz factors. Afterglow shocks are highly "non-magnetized": The ratio of magnetic field to kinetic energy flux ahead of the shock is very small, $U_{B1}/n_1 m_p c^2 \sim 10^{-9}$, where U_{B1} and n_1 are the magnetic energy density and particle number density in the upstream rest-frame. This strongly suggests that the shock structure is determined by the upstream density and the shock Lorentz factor alone (e.g. Gruzinov 2001a). We therefore adopt the assumption that the shock structure approaches a well defined limit as $U_{B1}/n_1 m_p c^2 \rightarrow 0$, and that GRB afterglow shocks are approximately described by this limiting solution (see § 2.1 for a detailed discussion).

It may be noted here that the upstream density can be eliminated from the problem by measuring time in units of the (shock-frame proton) plasma time, $\omega_p^{-1} = (4\pi\gamma_s n_1 e^2/m_p \gamma_s)^{-1/2} = (4\pi n_1 e^2/m_p)^{-1/2}$, and measuring distances in units of the corresponding skin depth, $l_{sd} = c/\omega_p$. The shock is then completely specified by the dimensionless parameter $\gamma_s v_s/c$ (and the dimensionless mass ratio m_e/m_p ; the upstream pressure is assumed negligible). In this sense, GRB shocks may be considered "simple."

The synchrotron model of GRB afterglows requires a strong magnetic field and a population of energetic electrons to be present in the downstream. Optical observations (e.g. Zhang & Mészáros 2004), the clustering of explosion energies (Frail et al. 2001), and the observed X-ray luminosity

¹ Physics Faculty, Weizmann Institute, Rehovot 76100, Israel; boazka@wizemail.weizmann.ac.il, waxman@wicc.weizmann.ac.il

² Institute for Advanced Study, Einstein Drive, Princeton, NJ 08540, USA; Friends of the Institute for Advanced Study member; keshet@sns.ias.edu

(Freedman & Waxman 2001; Berger et al. 2003) suggest that the fraction of post-shock thermal energy density carried by non-thermal electrons, ϵ_e , is large, $\epsilon_e \approx 0.1$. The fraction of post-shock thermal energy carried by the magnetic field, ϵ_B , is less well constrained by observations. However, in cases where ϵ_B can be reliably constrained by multi waveband spectra, values close to equipartition, $\epsilon_B \sim 0.01$ to 0.1 , are inferred (e.g. Frail, Waxman & Kulkarni 2000)³.

Near equipartition magnetic fields may conceivably be produced in the collisionless shock driven by the GRB explosion by electromagnetic (e.g. Weibel-like) instabilities (e.g. Blandford & Eichler 1987; Gruzinov & Waxman 1999; Medvedev & Loeb 1999; Wiersma & Achterberg 2004)⁴. The main challenge associated with the downstream magnetic field is related to the fact that in order to account for the observed radiation as synchrotron emission from accelerated electrons, the field amplitude must remain close to equipartition deep into the downstream, over distances $\sim 10^{10} l_{sd}$. At $t \sim 1$ d the magnetic field must be strong throughout the (proper) width $\Delta \sim 2\gamma_s c t \sim 10^{17}$ cm while $l_{sd} \sim 10^7 (n_1/1\text{cm}^{-3})^{-1/2}$ cm. This is a challenge since electromagnetic instabilities are believed to generate (near-equipartition) magnetic fields with coherence length $L \sim l_{sd}$, and a field varying on such scale is expected to decay within a few skin-depths downstream (Gruzinov 2001a). This suggests that the correlation length of the magnetic field far downstream must be much larger than the skin depth, $L \gg l_{sd}$, perhaps even of the order of the distance from the shock (Gruzinov & Waxman 1999; Gruzinov 2001a).

Growth of the characteristic length scale by many orders of magnitude, from $L \sim l_{sd}$ to $L \gg l_{sd}$, is a strong indication of self-similarity. In regions where $L \gg l_{sd}$, which also imply that L is much larger than the Larmor radius of thermal protons ($L \gg R_{L,th} \sim \gamma_s m_p c^2 / eB \sim l_{sd} \epsilon_B^{-1/2}$), it is reasonable to assume that L is the only relevant length scale, and self-similarity is expected (see § 3 for a detailed discussion). The main goal of the current paper is to introduce and formulate the assumption of a self-similar collisionless shock structure, and to study some of its consequences.

Although our analysis is motivated by GRB afterglow observations, it may be relevant also for non-relativistic collisionless shocks, such as shocks in young supernova remnants (SNRs). In the past few years, high resolution X-ray observations have provided indirect evidence for the presence of strong magnetic fields, $\gtrsim 100 \mu\text{G}$, in the *non-relativistic* ($v_s \sim \text{few} \times 1000 \text{ km s}^{-1}$) shocks of young SNRs (see Bamba et al. 2003; Vink & Laming 2003; Völk et al. 2005). These fields extend to distances $D > 10^{17}$ cm $\sim 10^{10} l_{sd}$ downstream, and possibly even $\gtrsim 10^{16}$ cm upstream, of the shock. In resemblance to GRB's, such strong magnetic fields cannot result from the shock compression of a typical interstellar medium (ISM) magnetic field, $B_1 \sim \text{few } \mu\text{G}$. In SNRs, the discrepancy is somewhat less severe, $U_{B1}/n_1 m_p v_s^2 \lesssim 10^{-4}$, and the possibility that these magnetic fields are related to the large

³ Eichler & Waxman (2005) have pointed out that observations determine ϵ_e and ϵ_B only up to a factor f , the fraction of electrons accelerated, where $m_e/m_p < f < 1$. However, it is expected that f is not very small, $f \gtrsim 1/10$ (Eichler & Waxman 2005).

⁴ It should be noted here that if a hydrodynamic description of the shock were applicable, the shock would have been stable and no magnetic fields could have been generated (Gruzinov 2000; Wang et al. 2002). A possible caveat is the presence of large inhomogeneities in the upstream plasma (ISM), which may drive turbulence in the downstream plasma, which may generate strong magnetic fields with large correlation length

scale ISM fields cannot be ruled out. If the ISM magnetic fields can be neglected, this suggests that these shocks too may have a self-similar nature. Henceforth, when discussing non-relativistic shocks, we assume that this is indeed the case.

The non-thermal energetic electron (and proton) population is believed to be produced by the diffusive (Fermi) shock acceleration (DSA) mechanism (for reviews see Drury 1983; Blandford & Eichler 1987; Malkov & Drury 2001). Acceleration of charged particles to high, non-thermal energies is a ubiquitous phenomenon in both relativistic and non-relativistic collisionless shocks. The accelerated particles are estimated to carry a considerable part of the energy: electrons alone carry $\sim 10\%$ of the thermal energy in GRB external shocks (Eichler & Waxman 2005) and $\sim 5\%$ of the thermal energy in SNR shocks (Keshet et al. 2004, and references therein); and at least 10% of the energy in SNR shocks must be converted into relativistic protons if these shocks are responsible for Galactic cosmic rays (Drury et al. 1989). This has several important implications. The accelerated particles are likely to have an important role in generating and maintaining the inferred magnetic fields. This conclusion is supported also by the evidence of strong amplification of the magnetic field in the upstream of GRB afterglow shocks (Li & Waxman 2006), which is most likely due to the streaming of high energy particles ahead of the shock. Since the high energy particles are likely to play an important role in the generation of the fields, a theory of collisionless shocks must provide a self-consistent description of particle acceleration, which depends on the scattering of these particles by magnetic fields, and field generation, which is likely driven by the accelerated particles.

The search for a self-consistent theory of collisionless shocks has led to extensive numerical studies. Particle in cell (PIC) simulations were performed in one dimension (e.g. Dieckmann et al 2006), in two dimensions (2D; e.g. Wallace & Epperlein 1991; Kato 2005), in two spatial and three velocity dimensions (2D3V; e.g. Gruzinov 2001a,b; Medvedev et al. 2005) and in the past few years also in three dimensions (3D; e.g. Silva et al. 2003; Nishikawa et al. 2003; Frederiksen et al. 2004; Jaroschek et al. 2004; Spitkovsky 2005). Such simulations have provided compelling evidence that transverse, electromagnetic (Weibel-like) instabilities generate near-equipartition magnetic fields in pair (e^+e^-) plasma, and $\epsilon_B \gtrsim m_e/m_p$ magnetic fields in ion-electron plasma. However, 3D simulations are limited to very small simulation boxes, and at present can reliably probe small length scales no larger than ~ 100 electron skin-depths, and short time scales no longer than ~ 100 electron plasma times. Hence, there is only preliminary evidence for the existence of collisionless shocks in 3D, and only in a pair-plasma (Simulations of ion-electron plasma are forced to employ an effective, small proton to electron mass ratio, $\tilde{m}_p/m_e \lesssim 20$ with present computational resources, and the preliminary results thus obtained are not easily extrapolated to more realistic mass ratios). Obviously, the question of field survival and correlation length evolution on length scales $\gg l_{sd}$ are not yet answered. Similarly, highly energetic particles cannot be contained in the small simulation boxes used, so Fermi-like acceleration processes are suppressed. It is important to note, that some published results are based on PIC simulations in stages where the boundary conditions strongly modify the plasma evolution. For example, claims that the magnetic fields decay slowly or saturate at some finite level remain questionable, until verified by simulations with sufficiently large simulation

boxes. A discussion of 3D PIC simulations and their physical implication appears in Appendix § A.

In § 2 we lay the basis for our analysis of afterglow (relativistic) and SNR (non-relativistic) shocks. In § 2.1 we discuss our assumption that these shocks are highly "non-magnetized," i.e. that the shock structure approaches a well defined limit as $U_{B1}/n_1 m_p v_s^2 \rightarrow 0$ and that the shocks observed are approximately described by this limiting solution. In § 2.2 we present the governing equations and discuss their dependence on dimensional parameters, which is relevant for the discussion of self-similarity. In particular, we demonstrate that when distances are measured in units of l_{sd} , the shock structure depends only on $\gamma_s v_s/c$ (and m_e/m_p). In § 2.3 we clarify the notion of "shock structure:" Since the electromagnetic fields and particle distributions fluctuate with time (at any given point downstream, and perhaps also upstream of the shock), the "stationary shock structure" is given by the correlation functions of the fluctuating quantities (which are expected to depend only on the distance from the shock). We define a notation that is useful for the discussion of the self-similarity assumption.

In § 3 we introduce and formulate the assumption of a self-similar structure in the downstream of non-magnetized collisionless shocks, derive several scaling relations of the physical quantities, and discuss some of the physical implications. One of the conclusions of § 3 is that the plasma may be approximately described as a combination of two self-similar components: a kinetic component of energetic particles, and an MHD-like component representing the bulk, "thermal" particles. The MHD-like component is discussed in § 4. We argue that this component may be treated as an infinitely conducting fluid, and show that this leads to a complete determination of the scaling laws.

In § 5 we present various extensions of the analysis. Self-similarity is studied in the upstream of non-magnetized collisionless shocks and in homogenous time-dependent plasmas, which may be more accessible to simulations than (non-homogeneous) collisionless shocks. In § 6 we discuss some of the implications of the self-similarity assumption to models of diffusive particle acceleration, and to the phenomenological model, suggested by Medvedev et al. (2005), of field generation through hierarchical merger of electric current filaments. The latter model is generalized, and shown to follow the self-similar scalings. Our main results and conclusions are summarized in § 7.

2. NON-MAGNETIZED COLLISIONLESS SHOCKS

2.1. Do non-magnetized collisionless shocks exist?

In general, the parameters determining the structure of a collisionless shock (for a given homogenous upstream composition which we assume to be an electron-proton plasma) are the shock (four) velocity $\gamma_s v_s$, and the upstream density n_1 , pressure P_1 and magnetic field \mathbf{B}_1 . We can formally ask what the limiting configuration is when \mathbf{B}_1 and P_1 approach zero. We assume that in this limit there is some shock solution, to which we refer as non-magnetized and strong. It is important to stress that by "non-magnetized" ("strong") we refer to the null effect of the value of the upstream magnetic field (pressure) on the stationary configuration of the shock, regardless of the dynamical role of these parameters in the generation of the shock.

We next ask how small should \mathbf{B}_1 and P_1 be so that the solution is no longer affected by their value. The dimension-

less parameters $\sigma_B = U_{B1}/n_1 m_p v_s^2, \sigma_P = P_1/n_1 m_p v_s^2$ measure the relative contribution of the magnetic field and thermal energy to the energy flux in the shock frame (which is constant and thus equal to its value in the far upstream),

$$T^{0z} \sim \gamma_s^2 n_1 m_p v_s^2 (1 + \sigma_B + \sigma_P) v_s, \quad (1)$$

where we assumed that the shock normal (the direction of the flow) is in the $\hat{\mathbf{z}}$ direction. It is reasonable to assume that if σ_B and σ_P are much smaller than unity, the magnetic field and pressure do not affect the shock structure. Since $\sigma_B \sim (l_{sd}/R_{L,th})^2$, the condition $\sigma_B \ll 1$ implies that the thermal protons in the shock frame are not affected by the compressed upstream magnetic field on the dynamical distance $\sim l_{sd}$ (the cyclotron time $\sim \gamma_s m_p c/eB$ is longer than the dynamical time $\sim \omega_p^{-1}$ as long as $\sigma_B < (c/v_s)^2$).

Simulations of relativistic shocks with various values of the upstream magnetic field (for a shock with Lorentz factor $\Gamma = 30$ in electron-positron plasma) are reported in Spitkovsky (2005), and a typical value of $\sigma_B \sim 10^{-2}$ is found to distinguish between the regimes of magnetized and non-magnetized shocks. Note, that this result may change considerably for electron-ion plasmas or if a population of accelerated particles is included, and may be affected by the transverse (perpendicular to the flow) boundary conditions (see § A). There is some debate regarding our assumption that the magnetic field in the upstream of GRB external shocks is insignificant. Lyubarsky & Eichler (2005) claim that the initial stages of the generation of the shock depend on the upstream magnetic field, because it can isotropize the protons faster than the magnetic fields generated in the shock can. Note, however, that even if the upstream magnetic field does play an important dynamical role in the evolution of the shock, this does not imply that the steady-state solution depends on the exact value of the upstream magnetic field.

Similarly, Bell (2004, 2005) and Milosavljevic & Nakar (2005b) claim that the cosmic ray precursor of the shock can amplify the upstream magnetic field significantly. Assuming that the magnetic field is amplified by many orders of magnitude, it is reasonable to assume that its initial value is not important.

2.2. Governing equations and dimensional considerations

Henceforth, we assume that strong, non-magnetized collisionless shocks do indeed exist. We consider a quasi steady-state planar shock. First, we consider the equations that govern the full plasma distribution function, $f_\alpha(\mathbf{x}, \mathbf{p}, t)$, and are valid globally, i.e. both upstream and downstream. Subscripts $\alpha \in \{e, i\}$ denote electrons and ions, respectively. Approximate equations, which are valid only in the far downstream and for which self-similarity is assumed, are discussed in § 3.3 and § 4.1.

The flow is governed by Vlasov's equation,

$$\partial_t f_\alpha + \mathbf{v}(\mathbf{p}) \cdot \nabla f_\alpha + q_\alpha \left(\mathbf{E} + \frac{1}{c} \mathbf{v} \times \mathbf{B} \right) \cdot \nabla_{\mathbf{p}} f_\alpha = 0, \quad (2)$$

and Maxwell's equations,

$$\begin{aligned} \nabla \times \mathbf{B} &= \frac{4\pi}{c} \mathbf{j} + \frac{1}{c} \partial_t \mathbf{E}, \\ \nabla \times \mathbf{E} &= -\frac{1}{c} \partial_t \mathbf{B}, \end{aligned} \quad (3)$$

where the electric current is related to f_α through

$$\mathbf{j} = \sum_\alpha q_\alpha \int d^3 \mathbf{p} \mathbf{v}(\mathbf{p}) f_\alpha(\mathbf{p}). \quad (4)$$

The velocity of the particles is given in terms of the momentum by

$$\mathbf{v}(\mathbf{p}) = c \frac{\mathbf{p}}{\sqrt{m_\alpha^2 c^2 + p^2}}. \quad (5)$$

As usual, the equations $\nabla \cdot \mathbf{B} = 0$ and $\nabla \cdot \mathbf{E} = 4\pi\rho$ are assumed to hold at some initial time, and are therefore preserved by the other equations at all times.

The shock is completely defined by the far upstream boundary conditions. Written in the shock frame, these conditions are

$$\begin{aligned} \mathbf{E}(D \rightarrow -\infty) &= \mathbf{B}(D \rightarrow -\infty) = 0, \\ f_\alpha(D \rightarrow -\infty) &= \gamma_s n_1 \delta^3(\mathbf{p} - \gamma_s \mathbf{v}_s m_\alpha \hat{\mathbf{z}}), \end{aligned} \quad (6)$$

where D is the distance from the shock front in the direction of the downstream (D is negative in the upstream). Note that the equations are independent of the frame of reference.

In order to highlight the dimensional dependencies of the Vlasov-Maxwell equations, we express the physical quantities $A = t, \mathbf{x} \dots$ in term of dimensionless variables \check{A} ,

$$\begin{aligned} t &= \frac{l_{sd}}{v_s} \check{t}, \quad \mathbf{x} = l_{sd} \check{\mathbf{x}}, \quad \mathbf{p} = \frac{m_\alpha}{m_p} p_{th} \check{\mathbf{p}}, \\ \mathbf{B} &= \frac{p_{th} c}{e l_{sd}} \check{\mathbf{B}}, \quad \mathbf{E} = \frac{p_{th} v_s}{e l_{sd}} \check{\mathbf{E}}, \\ \mathbf{j} &= e v_s \gamma_s n_1 \check{\mathbf{j}}, \end{aligned} \quad (7)$$

and

$$f_\alpha = \frac{\gamma_s n_1}{\left(\frac{m_\alpha}{m_p} p_{th}\right)^3} \check{f}_\alpha, \quad (8)$$

where

$$\begin{aligned} \omega_{pi}^2 &= \frac{4\pi n_1 e^2}{m_p} \sim \frac{4\pi n_2 e^2}{\gamma_s m_p}, \\ l_{sd} &= \frac{c}{\omega_{pi}}, \\ p_{th} &= m_p \gamma_s v_s, \end{aligned} \quad (9)$$

are the characteristic ion plasma frequency (squared), ion skin-depth and characteristic momentum of thermal particles in the downstream. Inserting these into Eqs. (2) and (3), we obtain

$$\begin{aligned} \partial_{\check{t}} \check{f}_\alpha + \frac{\mathbf{v}}{v_s} \cdot \check{\nabla} \check{f}_\alpha + \frac{q_\alpha/e}{m_\alpha/m_p} \left(\check{\mathbf{E}} + \frac{\mathbf{v}}{v_s} \times \check{\mathbf{B}} \right) \cdot \nabla_{\check{p}} \check{f}_\alpha &= 0, \\ \check{\nabla} \times \check{\mathbf{B}} &= \check{\mathbf{j}} + \frac{v_s^2}{c^2} \partial_{\check{t}} \check{\mathbf{E}}, \\ \check{\nabla} \times \check{\mathbf{E}} &= -\partial_{\check{t}} \check{\mathbf{B}} \end{aligned} \quad (10)$$

and

$$\check{\mathbf{j}} = \sum_\alpha \frac{q_\alpha}{e} \int d^3 \check{\mathbf{p}} \frac{\mathbf{v}}{v_s} \check{f}_\alpha, \quad (11)$$

with

$$\frac{\mathbf{v}}{v_s} = \frac{\check{\mathbf{p}}}{\sqrt{\frac{1}{\gamma_s^2} + \frac{v_s^2}{c^2} \check{p}^2}}. \quad (12)$$

The boundary conditions at upstream infinity (written in the shock frame) can similarly be written in dimensionless form,

$$\check{\mathbf{E}}(\check{D} \rightarrow -\infty) = \check{\mathbf{B}}(\check{D} \rightarrow -\infty) = 0 \quad (13)$$

and

$$\check{f}_\alpha(\check{D} \rightarrow -\infty) = \delta^3(\check{\mathbf{p}} - \check{\mathbf{z}}), \quad (14)$$

where $\check{D} = D/l_{sd}$.

Measuring distances in units of l_{sd} , we have thus arrived at a set of dimensionless equations, Eqs. (10)-(14), which depend only on $\gamma_s v_s/c$ (and on m_e/m_p).

2.3. Stationary shock structure

The electromagnetic fields and particle distributions at any given point behind (downstream of) the shock fluctuate with time. For each set of values of the shock parameters, n_1 and $\gamma_s v_s$, there is a large ensemble of time-dependent "specific solutions," with specific temporal and spatial dependence of particle distribution functions and electromagnetic fields. We assume that the averages and correlation functions of the fluctuating quantities depend only on the distance from the shock, and are identical for all specific solutions (in the limit that the size of the shock plane is infinite).

Consider for example the particle distribution function $f_\alpha(\mathbf{x} = D\hat{\mathbf{z}} + \mathbf{x}_\perp, \mathbf{p}, t)$ or magnetic field $\mathbf{B}(\mathbf{x} = D\hat{\mathbf{z}} + \mathbf{x}_\perp, t)$, where we have separated the \mathbf{x} dependence to dependence on the distance from the shock front, using $\hat{\mathbf{z}}$ as the direction of the shock normal, and on \mathbf{x}_\perp , a two dimensional vector perpendicular to $\hat{\mathbf{z}}$. While f_α depends on t and \mathbf{x}_\perp , we assume that an average of f_α over planes perpendicular to the shock normal is independent of t and \mathbf{x}_\perp :

$$\langle f_\alpha \rangle(\mathbf{p}; D) \equiv \lim_{r \rightarrow \infty} \frac{1}{\pi r^2} \int_{x'_\perp < r} d^2 \mathbf{x}'_\perp f_\alpha(D\hat{\mathbf{z}} + \mathbf{x}_\perp + \mathbf{x}'_\perp, \mathbf{p}, t). \quad (15)$$

Similarly, we assume that correlation functions of f, B and E may be defined, which are independent of t and \mathbf{x}_\perp , e.g.

$$\begin{aligned} B_{ij}(\Delta \mathbf{x}, \Delta t, D) &\equiv \\ &\lim_{r \rightarrow \infty} \frac{1}{\pi r^2} \int_{x'_\perp < r} d^2 \mathbf{x}'_\perp \\ &B_i[D\hat{\mathbf{z}} + \mathbf{x}_\perp + \mathbf{x}'_\perp, t] B_j[D\hat{\mathbf{z}} + \mathbf{x}_\perp + \Delta \mathbf{x} + \mathbf{x}'_\perp, t + \Delta t]. \end{aligned} \quad (16)$$

The stationary shock structure is described by $\langle f_\alpha \rangle$ and by the (infinite) set of correlation functions. Note, that the Maxwell-Vlasov equations may be converted to an (infinite) hierarchy of equations for the correlation functions.

It is useful for the analysis that follows to define the two-dimensional power spectrum of the magnetic field in a plane parallel to the shock front. We define the 2D power spectrum at distance D as

$$B_{ij}^{(2D)}(\mathbf{k}_\perp, D) \equiv (2\pi)^{-1} \int d^2 \mathbf{x}'_\perp B_{ij}(\mathbf{x}'_\perp, D) e^{i\mathbf{k}_\perp \cdot \mathbf{x}'_\perp}, \quad (17)$$

where $B_{ij}(\mathbf{x}'_\perp, D) \equiv B_{ij}(\Delta \mathbf{x} = \mathbf{x}'_\perp, \Delta t = 0, D)$. The plane averaged magnetic energy density is related to the correlation function by

$$\begin{aligned} \langle U_B \rangle(D) &= (8\pi)^{-1} \sum_i (2\pi)^{-1} \int d^2 \mathbf{k}_\perp B_{ii}^{(2D)}(\mathbf{k}_\perp, D) \\ &= (8\pi)^{-1} \sum_i B_{ii}(\Delta \mathbf{x} = 0, \Delta t = 0, D). \end{aligned} \quad (18)$$

Note that the plane-averaged magnetic field vanishes. As a consequence of the planar symmetry, a non-zero averaged magnetic field would be oriented along the z -axis. As its divergence vanishes, the magnitude of $\langle \mathbf{B} \rangle$ would be constant and thus equal to its far upstream value which is zero. The root mean square (rms) magnetic field,

$$\bar{B}(D) = \left[\sum_i B_{ii}(\Delta \mathbf{x} = 0, \Delta t = 0, D) \right]^{1/2}, \quad (19)$$

serves as a measure of the characteristic magnetic field amplitude at a distance D from the shock (note, $\langle U_B \rangle = \bar{B}^2/8\pi$).

3. SELF-SIMILARITY IN THE DOWNSTREAM

As discussed in the introduction, afterglow observations suggest that the characteristic length scale L for variations in the magnetic field becomes much larger than l_{sd} , $L \gg l_{sd}$, at distances $D \gg l_{sd}$ downstream of the shock. We assume here that in the limit $L/l_{sd} \rightarrow \infty$, L becomes the only length scale relevant for the evolution of the plasma, which implies self-similarity. There is no proof that self-similarity will be present whenever the characteristic length scale diverges (or becomes infinitesimal). However, the self-similarity assumption is known to be valid for many physical systems in which such divergence occurs [see, e.g., Zeldovich & Raizer (1968) for self-similarity in hydrodynamics, and Kadanoff et al. (1967) for self-similarity in critical phenomena]. In order to clarify the reasoning behind this assumption and its implications, we first briefly describe in § 3.1 an example of a physical system, where the presence of a diverging characteristic length scale leads to self-similar behavior. We then formulate in § 3.2 the self-similarity assumption for the downstream of collisionless shocks. The separation of the plasma into two components is discussed in § 3.3. The scaling relations are derived in § 3.4, and some of their implications are discussed in § 3.5.

A note is in place here regarding non-relativistic collisionless shocks. As mentioned in the introduction, self-similarity may be expected in the non-relativistic shocks observed in young SNR's. The analysis is similar for relativistic and non-relativistic shocks, and in particular leads to the same scaling relations and implications. The main difference is that in the non-relativistic case there is a physically relevant length scale, which is different than the skin depth l_{sd} : The Larmor radius of mildly relativistic protons, $R_L \sim m_p c^2/eB \sim R_{L,th}(v_s/c)^{-1} \sim (v_s/c)^{-1} l_{sd}$, where $R_{L,th}$ is the characteristic Larmor radius of thermal protons. In other words, there is a small parameter in the problem, (v_s/c) , which is likely to have a physical implication. Hence, although in this case too we expect self-similarity as $L/l_{sd} \rightarrow \infty$, we expect the self-similar solution to provide a good approximation for $L \gg (v_s/c)^{-1} l_{sd}$ rather than for $L \gg l_{sd}$, and the scaling relations of the particle distribution functions to be valid for momenta $p > m_p c$.

3.1. An example of self-similarity

Consider a macroscopic system in thermodynamic equilibrium, exhibiting a phase transition at some temperature T_c . Near the critical temperature, $T \sim T_c$, the correlation length L of fluctuations within the system diverges, $L(\delta T) \rightarrow \infty$ as $\delta T \equiv T - T_c \rightarrow 0$. It is commonly assumed that in this limit L becomes the only "relevant" length scale, and that the microscopic length scales, e.g. the inter-particle distance d , become irrelevant.

To clarify this assumption, let us consider the correlation function $f(r)$ of some fluctuating quantity. f is a function

of δT and of the various parameters defining the thermodynamic system (e.g. d). Assuming L diverges monotonically with δT we may replace the dependence on δT with dependence on L , $f(r; L, d, c_i)$ where c_i represent the parameters defining the thermodynamic system. We may assume that these parameters contain no parameter with the dimensions of length, since any such parameter c_k may be replaced by a dimensionless parameter, c_k/d . Using the dimensional parameters, a constant A_f with the same dimensions of f may be constructed, and f may be written as $f = A_f \tilde{f}$ where \tilde{f} is a dimensionless function. Since \tilde{f} is dimensionless, it must be a function of only dimensionless combinations of $\{r, L, d, c_i\}$. Thus, $f = A_f \tilde{f}(r/L; d/L, \tilde{c}_i)$ where \tilde{c}_i represent the dimensionless combinations of c_i . As L/d diverges it is assumed that d becomes "irrelevant," in the sense that \tilde{f} approaches a limit

$$f(r; L, d, c_i) = A_f \tilde{f} \left(\frac{r}{L}; \frac{d}{L}, \tilde{c}_i \right) \xrightarrow{d/L \rightarrow 0} A_f \left(\frac{d}{L} \right)^{-s_f} \tilde{g} \left(\frac{r}{L}; \tilde{c}_i \right). \quad (20)$$

Note, that it is not assumed that, as $d/L \rightarrow 0$, \tilde{f} approaches a limit independent of d/L , but rather that in this limit it has a scale-free (power-law) dependence on d/L . In the former case, f depends on the dimensional parameters A_f and L alone, and in the latter on $A_f d^{-s_f}$ and L . In both cases, the only length scale that may be extracted from f is L . Similar arguments lead to the conclusion that L has a power-law dependence on δT ,

$$\delta T(L, d, c_i) = T_c \delta T \left(\frac{d}{L}, \tilde{c}_i \right) \xrightarrow{d/L \rightarrow 0} T_c \left(\frac{d}{L} \right)^{-s_{\delta T}} \tilde{h}(\tilde{c}_i). \quad (21)$$

In general, the self-similarity assumption may be stated as the assumption that all the properties of the system at some $\delta T = \delta T_1$, corresponding to $L_1 = L(\delta T_1)$, are identical to those of the system at $\delta T = \delta T_2$, corresponding to $L_2 = L(\delta T_2)$, up to a scaling transformation. That is, any function describing some properties of the system, e.g. $f[r, \delta T(L)]$, is identical at L_1 and L_2 up to a scaling of r and f ,

$$f(r, L_2) = \left(\frac{L_2}{L_1} \right)^{s_f} f \left(\frac{r}{L_2/L_1}, L_1 \right) \quad (22)$$

for some s_f . The function f is termed self-similar, as it is similar to itself at different L values. Comparing Eqs. (22) and (20) it is clear that the assumption that d is "irrelevant" is equivalent to the assumption that f is self-similar.

It is clear from the above example that the assumption of self-similarity provides powerful constraints on the properties of the system, and that a complete characterization of its properties requires determination of the similarity exponents $\{s_f, s_{\delta T}\}$.

3.2. The self-similarity assumption

Consider the plasma at a distance $D \gg l_{sd}$ downstream of the shock, where the field correlation length is assumed to satisfy $L \gg l_{sd}$. Assuming L/l_{sd} diverges with D , we expect the structure of the shock to become self-similar. That is, we expect the averaged distribution function $\langle f_\alpha \rangle$, the rms magnetic field \bar{B} and the (infinite) set of correlation functions to be self-similar:

$$\bar{B}(L) = \left(\frac{L}{L_0} \right)^{s_B} \bar{B}(L_0), \quad (23)$$

$$\langle f_\alpha \rangle(\mathbf{p}, L) = \left(\frac{L}{L_0} \right)^{s_f} \langle f_\alpha \rangle \left[\frac{\mathbf{p}}{(L/L_0)^{s_p}}, L_0 \right], \quad (24)$$

$$B_{ij}(\Delta \mathbf{x}, \Delta t, L) = \left(\frac{L}{L_0} \right)^{2s_B} B_{ij} \left[\frac{\Delta \mathbf{x}}{L/L_0}, \frac{\Delta t}{(L/L_0)^{s_i}}, L_0 \right], \quad (25)$$

and so on, where L_0 is a reference length scale. Note, that we have replaced the dependence on D with a dependence on L , assuming that L diverges monotonically with D .

The values of the similarity exponents are not determined by the requirement of self-similarity alone, and must be derived based on additional arguments. In what follows, we derive constraints on the similarity exponents $\{s_i, s_p, s_B, \dots\}$ using the Maxwell-Vlasov equations. Since self-similarity applies to averaged quantities, e.g. $\langle f_\alpha \rangle$ and B_{ij} , rather than to specific solutions, this derivation should be based on the equations for the averaged quantities, which are obtained from the Maxwell-Vlasov equations. Such a derivation is, however, rather cumbersome. Identical constraints on the similarity exponents may be derived in a simpler way by assuming that the specific solutions form a scalable family in the sense that if $\{f_\alpha(\mathbf{x}, \mathbf{p}, t), \mathbf{B}(\mathbf{x}, t)\}$ is a solution of the Maxwell-Vlasov equations, then the scaled functions

$$\begin{aligned} \mathbf{B}'(\mathbf{x}, t) &= \xi^{s_B} \mathbf{B} \left(\frac{\mathbf{x}}{\xi}, \frac{t}{\xi^{s_i}} \right), \\ f_\alpha'(\mathbf{x}, \mathbf{p}, t) &= \xi^{s_f} f_\alpha \left(\frac{\mathbf{x}}{\xi}, \frac{\mathbf{p}}{\xi^{s_p}}, \frac{t}{\xi^{s_i}} \right), \end{aligned} \quad (26)$$

also constitute a solution (at least approximately). It is straightforward to verify that the self-similarity requirements, Eqs. (24)-(25), are automatically satisfied under this assumption, by substituting $\xi = L/L_0$ in Eq. (26) and recalling that the averages and correlation functions are identical for all specific solutions. Under the assumption that the solutions are scalable, we can use the Maxwell-Vlasov equations directly (instead of the equations for the correlation functions) in order to derive the constraints on the similarity exponents. Before doing so, we address (in § 3.3) the separation of the plasma into two components.

It is important to emphasize here, that although the constraints derived under the assumption that the solutions are scalable (in the above sense) are identical to those derived from the self-similarity requirements, Eqs. (24)-(25), it is not obvious that the self-similarity requirements indeed imply that the specific solutions are scalable.

3.3. Two plasma components

As the plasma flows away from the shock, most of the particles remain "thermal,"⁵ i.e. most protons carry a momentum $\sim p_{th}$ (and most electrons carry a momentum $(m_e/m_p)^\nu p_{th}$ with $\nu \geq 0$). This implies the existence of a length scale $R_{L,th}(L) = p_{th}c/e\bar{B} \propto L^{-s_B}$, $R_{L,th}/L \propto L^{-(1+s_B)}$. Obviously, in order for L to be the only relevant scale, we must have $s_B > -1$. Combined with the requirement that the field energy density does not diverge we have

$$-1 < s_B \leq 0. \quad (27)$$

Our assumption that L is the only relevant length scale implies that $R_{L,th}$ is irrelevant. However, $R_{L,th}$ is obviously relevant for the description of the microscopic motion of individual "thermal" particles. This apparent contradiction may

⁵ The term "thermal" is used for convenience to describe particles with kinetic energy $\sim (\gamma_s - 1)m_p c^2$. In what follows, it is not claimed or assumed that the energy distribution of these particles is thermal i.e. a (relativistic) Maxwellian distribution.

be resolved only if the microscopic motion of "thermal" particles, i.e. of particles with momenta p such that $pc/e\bar{B} \ll L$, is unimportant. These particles should therefore be described by effective equations, where the microscopic particle motion is unimportant. We leave the discussion of the "thermal" particles, to which we refer henceforth as the "fluid" particles, to § 4, and note here only several points which are important for the discussion that follows.

First, the scaling of f_α derived in the previous section does not apply to all particle momenta, but rather to the large p , $p \gg p_{th}(v_s/c)^{-1}$, behavior of f_α . In particular, the Vlasov equation in this region, where $\mathbf{v}(\mathbf{p}) \approx c\hat{\mathbf{p}}$, can be written as,

$$\partial_t f_\alpha + c\hat{\mathbf{p}} \cdot \nabla f_\alpha + q_\alpha \left(\mathbf{E} + \frac{1}{c} \mathbf{v} \times \mathbf{B} \right) \cdot \nabla_{\mathbf{p}} f_\alpha = 0. \quad (28)$$

Second, the total electric current is the sum of the electric currents carried by the high energy particles, \mathbf{j}_h , and by the "fluid," \mathbf{j}_F , $\mathbf{j} = \mathbf{j}_h + \mathbf{j}_F$. Hereafter, h and F subscripts refer to the high energy and to the fluid particles, respectively. The electric current \mathbf{j}_h is given by

$$\mathbf{j}_h = \sum_\alpha q_\alpha \int_{p > \xi_p e\bar{B}L/c} d^3 \mathbf{p} c \hat{\mathbf{p}} f_\alpha(\mathbf{p}). \quad (29)$$

Here, $\xi_p(L)$ is a dimensionless function that determines the threshold momentum between accelerated and fluid components. It must satisfy $\xi_p > (v_s/c)^{-1} p_{th}c/e\bar{B}L = (v_s/c)^{-1} R_{L,th}/L$ in order to ensure that the accelerated component is not affected by the thermal scale. It must also tend to zero as L diverges, as self-similarity is expected for all scales $\gg (v_s/c)^{-1} R_{L,th}$.

Solutions of the type we have arrived at, where the self-similar solution describes the evolution in some part of $(\mathbf{x}, \mathbf{p}, t)$ phase space while the other part is described by a different solution, are usually called "second type solutions" (e.g. Zeldovich & Raizer 1968; Waxman & Shvarts 1993). In second type solutions, the similarity exponents can not be determined by global conservation laws. For example, one may have argued that a relation between s_f and s_p may be derived by requiring the integral over momenta of $\langle f \rangle$, given by Eq. (24), to be equal to the (downstream) particle density,

$$n_\alpha = \int d^3 p \langle f_\alpha \rangle(\mathbf{p}, L) = \left(\frac{L}{L_0} \right)^{3s_p + s_f} \int d^3 y \langle f_\alpha \rangle(\mathbf{y}, L_0), \quad (30)$$

which would imply $3s_p + s_f = 0$. Such a constraint can not be derived, however, since the scaling relation, Eq. (24), used for obtaining the second equality of Eq. (30) does not hold for small values of y . In fact, as we show below, the functional form of f derived by the self-similarity arguments is such that the integral on the rhs of Eq. (30) diverges at small y . The number of particles described by the self-similar solution does not diverge, however, since the integration extends only down to $y = \xi_p(L)(L/L_0)^{1-s_p} e\bar{B}L_0/c$ (note, that this constrains the dependence of ξ_p on L). This is analogous to the divergence of energy in second-type self-similar solutions of hydrodynamic flows (e.g. Waxman & Shvarts 1993).

The particles with $p \lesssim \xi_p(L)e\bar{B}L/c$ are described by a solution different than the self-similar solution describing the higher momenta, "accelerated," particles. As in any second type self-similar solution, it is necessary that the non self-similar part of the solution does not affect the self-similar part (this requirement often determines the similarity exponents of second type solutions, e.g. Zeldovich & Raizer 1968; Waxman & Shvarts 1993). In our case, the particles

at $p \lesssim \xi_p(L)e\bar{B}L/c$ may affect the higher momentum particles only through their contribution to the electric current. This implies that the current contributed by $p \lesssim \xi_p(L)e\bar{B}L/c$ particles must either be negligible or scale with L in a similar way as the current of the higher momenta particles does. For the fluid current, this requirement implies that either $j_F \ll j_h$ or $j_F(L)/j_h(L) \propto L^0$. In addition, this requirement implies that the integral on the rhs of Eq. (29) converges (as otherwise the current would be dominated by $p \lesssim \xi_p(L)e\bar{B}L/c$ particles).

The following point should be emphasized here. We have implicitly assumed above that the high momenta, accelerated particles are dynamically important in the sense that their electric current makes a considerable contribution to the total electric current, $\mathbf{j}_h \sim \mathbf{j}$. However, self-similar solutions where the accelerated particles do not contribute to the current, $j_h \ll j$, are possible in principle. In this case, the growth of the magnetic field fluctuation correlation length should be driven by the fluid, and the accelerated particles can be treated as "test-particles," which do not affect the flow. As mentioned in the introduction, such a picture is unlikely, due to the fact that the accelerated particles carry a significant fraction of the energy and due to the evidence that they play a role in generating magnetic fields in the upstream plasma.

3.4. Scaling relations

Let us consider first the scaling of L with D . Since the characteristic length scale for changes in L is L , we must have $L \propto D$: Requiring the scale for changes in L to be proportional to L may be written as $d(\log L)/dD \propto 1/L$ which implies $L \propto D$. It should be noted that this assumption is not equivalent to assuming that the only length scale relevant for the evolution is D . Under such an assumption, $d(\log L)/dD = s/D$ implying $L = D^s$, which allows the possibility $L/D \rightarrow 0$ as $D \rightarrow \infty$.

Next, we consider the scaling of time, i.e. the value of s_t . Substituting the scaled solutions, Eqs. (26), into the Vlasov equation, Eq. (28), one finds that the various terms in the equation scale differently with ξ . In order for the scaling of the temporal and the spatial derivative terms to be similar, one must require $s_t = 1$. However, one can not conclude from this that $s_t = 1$ is the only value allowed, since it is possible that one of the first two terms, $\partial_t f$ or $\mathbf{v} \cdot \nabla f$, becomes negligible as $L \rightarrow \infty$, and may be neglected altogether in the Vlasov equation. Nevertheless, we conclude that $s_t = 1$ is required based on the following arguments. The case $s_t < 1$, implying that $cT/L \rightarrow 0$ as $L \rightarrow \infty$ where T is the characteristic time for variations in the physical quantities, is ruled out since it would imply that at large distances from the shock the electric field is much larger than the magnetic field ($E/B \rightarrow \infty$ as $L \rightarrow \infty$), which is inconsistent with the synchrotron model of afterglow emission. Assuming $s_t > 1$, $cT/L \rightarrow \infty$ as $L \rightarrow \infty$, would imply that at large distances from the shock the magnetic fields are approximately static (velocities of the field lines of the order L/T) in the shock frame. Once the condition $L/T \ll v_s$ would be reached, the thermal protons would gyrate around the static field lines (the gyration radius, $R_{L,th}$, is much smaller than L , and thus also the gyration time, $T_{L,th} \sim R_{L,th}/v_s$, is much shorter than T), in contradiction with the fact that the bulk downstream fluid moves with velocity $v_d \lesssim v_s$ (Note that $\gamma_d = (1 - v_d^2/c^2)^{-1/2} \sim 1$). We conclude that we must have $s_t = 1$.

The scaling of the momentum, i.e. the value of s_p , is determined by comparing the momentum derivative term with the spatial (or temporal) derivative term in the Vlasov equation.

Substituting the scaled solutions, Eqs. (26), into the Vlasov equation, Eq. (28), and requiring all terms to scale similarly implies $s_p = 1 + s_B$. One implication of this scaling is that the Larmor radius scales as L (in fact, the entire trajectory of each particle scales with L).

Finally, we derive the relation between s_f and s_B . The current provided by the accelerated particles is

$$\begin{aligned} \mathbf{j}'_h(\mathbf{x}, t) &= \sum_{\alpha} q_{\alpha} \int d^3 \mathbf{p} c \hat{\mathbf{p}} \xi^{s_f} f_{\alpha} \left(\frac{\mathbf{x}}{\xi}, \frac{\mathbf{p}}{\xi^{s_B+1}}, \frac{t}{\xi} \right) \\ &= \xi^{s_f+3(s_B+1)} \sum_{\alpha} q_{\alpha} \int d^3 \mathbf{p} c \hat{\mathbf{p}} f_{\alpha} \left(\frac{\mathbf{x}}{\xi}, \mathbf{p}, \frac{t}{\xi} \right) \\ &= \xi^{s_f+3(s_B+1)} \mathbf{j}_h \left(\frac{\mathbf{x}}{\xi}, \frac{t}{\xi} \right). \end{aligned} \quad (31)$$

We have not shown here explicitly the lower limit of the integration over p , since, as discussed in § 3.3, the current integral must converge at small p . Substituting the scaled current, and the scaled magnetic field, into Maxwell's equation, $\nabla \times \mathbf{B} = 4\pi c^{-1} \mathbf{j} + c^{-1} \partial_t \mathbf{E}$, we find that the $\nabla \times \mathbf{B}$ and \mathbf{j} terms scale similarly with ξ provided that $s_f + 3(s_B + 1) = s_B - 1$.

To summarize, in order for the scaled solutions, Eqs. (26), to satisfy the Vlasov-Maxwell equations, it is necessary (and sufficient) for the similarity indices to satisfy

$$s_t = 1, \quad s_p = s_B + 1, \quad s_f = -4 - 2s_B. \quad (32)$$

In addition, we have shown that $-1 < s_B \leq 0$ and that

$$L \propto D. \quad (33)$$

The relation between s_p and s_B implies that the Larmor radius of the particles scales as L . The relation between s_f and s_B implies that the energy density of accelerated particles in any momentum interval, $U_h = \sum_{\alpha} \int d^3 \mathbf{p} c p f_{\alpha}$, scales as the magnetic field energy density (when the momentum interval scales appropriately). Combining the above results, we find that $\langle U_h \rangle \propto \langle U_B \rangle \propto L^{2s_B} \propto D^{2s_B}$.

An illustration of the plasma configuration downstream of a hypothetical self-similar collisionless shock appears in Figure (1).

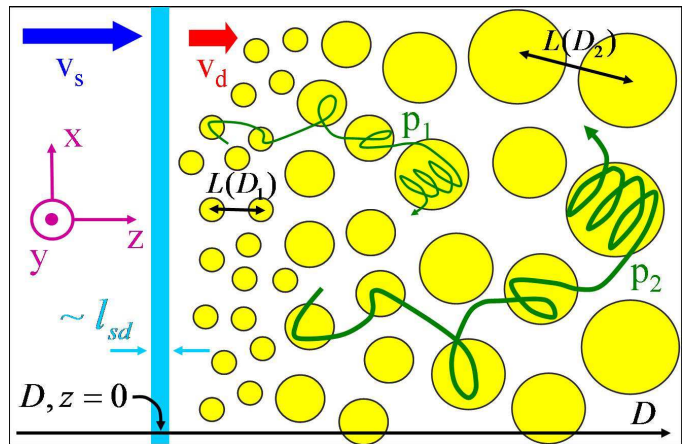


FIG. 1.— Schematic illustration of the model. The shaded vertical band at $D = z = 0$ represents the shock. Shaded Circles designate regions where the magnetic field amplitude B exceeds some constant threshold. The characteristic scale L for variations in B increases with distance D from the shock. Curved lines illustrate the trajectories of two high-energy particles of different momenta, $p_1 < p_2$, becoming magnetized ($R_L < L$) at two different scales.

3.5. Additional implications

The scaling relations derived above may be used to constrain the momentum dependence of the particle distribution functions. Using $L_0 = L(p_0/p)^{1/s_p}$ in Eq. (24) we obtain

$$\begin{aligned} \langle f_\alpha \rangle(\mathbf{p}, L) &= \left(\frac{p}{p_0}\right)^{s_f/s_p} \langle f_\alpha \rangle \left[\hat{\mathbf{p}} p_0, L \left(\frac{p_0}{p}\right)^{1/s_p} \right] \\ &\xrightarrow{p/p_0 \rightarrow \infty} \langle f_\alpha \rangle(\hat{\mathbf{p}} p_0, 0) \left(\frac{p}{p_0}\right)^{s_f/s_p}. \end{aligned} \quad (34)$$

This implies that $\langle f_\alpha \rangle(\mathbf{p}, L)$ approaches a power-law distribution at large p , $\langle f_\alpha \rangle(\mathbf{p}, L) \propto p^{s_f/s_p}$, provided that $\langle f_\alpha \rangle(\mathbf{p}, L)$ approaches a finite limit for some p as $L \rightarrow 0$. The condition that $\langle f_\alpha \rangle(\mathbf{p}, L) \rightarrow \text{Const} \neq 0$ as $L \rightarrow 0$ is equivalent to the requirement that accelerated particles reach the shock front. This is physically reasonable since cosmic rays are expected to reach the upstream. Moreover, it is a necessary condition for any acceleration process that involves the shock front (such as diffusive Fermi acceleration).

A similar constraint may be obtained by taking the limit $p/p_0 \rightarrow 0$, which yields

$$\begin{aligned} \langle f_\alpha \rangle(\mathbf{p}, L) &= \left(\frac{p}{p_0}\right)^{s_f/s_p} \langle f_\alpha \rangle \left[\hat{\mathbf{p}} p_0, L \left(\frac{p_0}{p}\right)^{1/s_p} \right] \\ &\xrightarrow{p/p_0 \rightarrow 0} \langle f_\alpha \rangle(\hat{\mathbf{p}} p_0, \infty) \left(\frac{p}{p_0}\right)^{s_f/s_p}. \end{aligned} \quad (35)$$

This implies that $\langle f_\alpha \rangle(\mathbf{p}, L)$ approaches a power-law distribution at small p , $\langle f_\alpha \rangle(\mathbf{p}, L) \propto p^{s_f/s_p}$, provided that $\langle f_\alpha \rangle(\mathbf{p}, L)$ approaches a finite limit for some p as $L \rightarrow \infty$. The condition that $\langle f_\alpha \rangle(\mathbf{p}, L) \rightarrow \text{Const} \neq 0$ as $L \rightarrow \infty$ is equivalent to the requirement that accelerated particles reach downstream infinity. This is physically reasonable since cosmic rays are expected to be advected with the flow to the downstream (e.g. in diffusive Fermi acceleration). Moreover, the presence of high energy electrons in the far downstream ($\sim 10^{10} l_{sd}$) is required to account for afterglow observations. Thus, we conclude that the self-similar distribution function approaches a power-law dependence on p at both high and low momenta,

$$\frac{dn_\alpha}{dp} \propto p^2 \int d^2 \hat{\mathbf{p}} f_\alpha(p \hat{\mathbf{p}}) \propto p^{-2/(s_B+1)}. \quad (36)$$

Let us consider next the magnetic field correlation function. Using $L/L_0 = \Delta x/\Delta x_0$ in Eq. (25) we obtain

$$\begin{aligned} B_{ij}(\Delta \mathbf{x}, \Delta t, L) &= \left(\frac{\Delta x}{\Delta x_0}\right)^{2s_B} B_{ij} \left[\Delta x_0 \hat{x}, \frac{\Delta t}{\Delta x/\Delta x_0}, \frac{\Delta x_0}{\Delta x} L \right], \\ &\xrightarrow{\Delta x/\Delta x_0 \rightarrow \infty} \left(\frac{\Delta x}{\Delta x_0}\right)^{2s_B} B_{ij}(\Delta x_0 \hat{x}, 0, 0), \end{aligned} \quad (37)$$

where \hat{x} is a unit vector in the direction of $\Delta \mathbf{x}$. This implies that $B_{ij}(\Delta \mathbf{x}, \Delta t, L)$ approaches a power-law behavior at large Δx , $B_{ij}(\Delta \mathbf{x}, \Delta t, L) \propto \Delta x^{2s_B}$, provided that $B_{ij}(\Delta \mathbf{x}, \Delta t, L)$ approaches a finite limit for some Δx_0 as $L, \Delta t \rightarrow 0$. This is expected to be the case under the assumption that the accelerated particles reach the shock front, since in this case the number of particles with Larmor radius greater than (some given) Δx approaches a constant as $L \rightarrow 0$, and such particles are expected to generate a correlation between the magnetic fields at points separated by $\Delta \mathbf{x}$.

Eq. (37) implies that the magnetic power spectrum has a component which scales as k^{-2-2s_B} . Assuming that the result $B_{ij}(\Delta \mathbf{x}, 0, L) \approx (\Delta x/\Delta x_0)^{2s_B} B_{ij}(\Delta x_0 \hat{x}, 0, 0)$ holds for $\Delta x >$

$\eta \Delta x_0$, where η is some dimensionless constant, the power spectrum may be written as (see § 2.3)

$$\begin{aligned} 2\pi B_{ij}^{(2D)}(\mathbf{k}_\perp, L) &\approx \int_{x'_\perp < \eta \Delta x_0} d^2 \mathbf{x}'_\perp B_{ij}(\mathbf{x}'_\perp, L) e^{-i\mathbf{k}_\perp \cdot \mathbf{x}'_\perp} \\ &+ (\Delta x_0)^{-2s_B} \int_{\eta \Delta x_0}^\infty dx'_\perp x'^{1+2s_B}_\perp \int_0^{2\pi} d\theta B_{ij}(\Delta x_0 \hat{\mathbf{x}}'_\perp, 0, 0) e^{-i\mathbf{k}_\perp \cdot \mathbf{x}'_\perp} \\ &= f_1(\mathbf{k}_\perp, \eta \Delta x_0, L) \\ &+ (\Delta x_0)^{-2s_B} k_\perp^{-2-2s_B} \int_{k_\perp \eta \Delta x_0}^\infty du u^{1+2s_B} \int_0^{2\pi} d\theta B_{ij}(\Delta x_0 \hat{\mathbf{u}}, 0, 0) e^{-i\mathbf{k}_\perp \cdot \mathbf{u}}, \end{aligned} \quad (38)$$

where, $\mathbf{u} \equiv k_\perp \mathbf{x}'_\perp$. In the long wavelength limit, $0 < k_\perp \ll (\eta \Delta x_0)^{-1}$, the exponent in f_1 is approximately constant, such that f_1 is nearly independent of \mathbf{k}_\perp . In addition, the lower limit in the second integral, $k_\perp \eta \Delta x_0$, may be taken to zero (recall that $s_B > -1$). Thus, $2\pi B_{ij}^{(2D)}(\mathbf{k}_\perp, L) \approx f_1(\eta \Delta x_0, L) + k_\perp^{-2-2s_B} f_2(\hat{\mathbf{k}}_\perp, \Delta x_0)$ where we assumed that the integral in the second term converges. As $s_B > -1$, for $k_\perp \rightarrow 0$ we can neglect f_1 so that

$$B_{ij}^{(2D)}(\mathbf{k}_\perp, L) \propto k_\perp^{-2-2s_B}. \quad (39)$$

The scaling of various other correlation functions, such as $\langle f_\alpha f_\beta \rangle$, may be deduced in the method shown above. For example, the arguments leading to the conclusion $B_{ij}(\Delta \mathbf{x}, \Delta t, L) \propto \Delta x^{2s_B}$ for $\Delta x \rightarrow \infty$ also imply that $B_{ij}(\Delta \mathbf{x}, \Delta t, L) \propto \Delta t^{2s_B}$ for $\Delta t \rightarrow \infty$.

4. THE "FLUID" COMPONENT, DOWNSTREAM

As explained in §3.3, the assumption that L is the only relevant scale implies that the microscopic motion of the thermal particles (referred to as the "fluid" particles) is unimportant for the global solution. One option is that the current carried by the fluid is negligible, $j_F \ll j_h$, in which case these particles do not affect the EM fields. The second option is that the current carried by this population is considerable $j_F \sim j_h \sim j$ (i.e. that it scales as the electric current carried by the accelerated component), and that the thermal fluid is described by effective equations independent of the microscopic scales l_{sd} and $R_{L,th} = p_{thc}/eB$. The first option is unlikely since, as we show in §4.2, the fluid is expected to be highly conducting and thus probably carries non-negligible currents. In this section we study the implications of the second option, $j_F \sim j_h$. We assume that the appropriate effective degrees of freedom are those of a single fluid, since the skin depth l_{sd} and thermal Larmor radius $R_{L,th}$ have an important role already at the level of two fluid equations.

In order to obtain equations which are independent of the downstream bulk velocity of the fluid, which can not scale with L , we consider the flow in the downstream frame (where the bulk velocity vanishes). Note, that since $s_t = 1$, the self similarity relations, e.g. Eqs. (26), hold both in the shock frame and in the downstream frame (and in any other frame, as long as we set $t = 0$ as the time when the shock was at $z = 0$). As the current carried by the fluid is non-negligible, $\mathbf{j}_F \sim \mathbf{j}$, it must have a self similar structure. We thus assume that all the dynamically important fluid quantities have a self similar structure. In particular, the fluid velocity field \mathbf{u} (in the downstream frame) scales as

$$\mathbf{u}'(\mathbf{x}, t) = \xi^{s_u} \mathbf{u}\left(\frac{\mathbf{x}}{\xi}, \frac{t}{\xi}\right). \quad (40)$$

In §4.2 we show, that for $L \gg R_{Lth}$ the fluid can be considered as infinitely conducting, i.e.

$$\mathbf{E} = -\frac{1}{c} \mathbf{u} \times \mathbf{B}. \quad (41)$$

This, together with Maxwell's equation $\nabla \times \mathbf{E} = -c^{-1} \partial_t \mathbf{B}$, implies that $L/T \sim u$ and thus $s_u = 1 - s_t = 0$. In other words, the velocity fluctuations scale trivially. In order to relate this to the magnetic field we consider the force density applied to the fluid, $\sim \gamma_s^2 n_1 m_p u/T$ where T is the characteristic time scale for variations. The force has a contribution from the pressure, $\sim P/L$ where P is the fluctuating part of the pressure, and from the EM fields, $\sim c^{-1} j_f B \sim U_B/L$ where U_B is the magnetic field energy density. If U_B is not negligible compared to P , requiring that the two force densities, $\gamma_s^2 n_1 m_p u/T$ and $c^{-1} j_f B \sim U_B/L$, scale similarly we find, using $u \propto L^0$ and $T \propto L^1$, that $s_B = 0$. If U_B is negligible, $P \gg U_B$, the force density is dominated by P/L and s_B can not be constrained by considering the force density scaling. However, $P \gg U_B$ is unlikely. Our basic assumption that the accelerated component plays an important role in the solution suggests that the fluctuations in the fluid are driven by it. As the interaction between the accelerated component and the fluid is mediated through the EM fields this implies that they have a considerable contribution to the force density applied to the fluid. Moreover, the observational evidence that ϵ_B is not very small, $\epsilon_B \sim 10^{-2} - 10^{-1}$, does not leave much room for P (which is smaller than U_B/ϵ_B) to be much larger than U_B . We conclude therefore that

$$s_u = s_B = 0, \quad (42)$$

which, using Eq. (32), implies

$$s_p = 1, \quad s_f = -4. \quad (43)$$

Eq. (42) and (43) imply that $U_u \propto U_B \propto U_h$, where U_u , U_B and U_h are the energy densities of the fluid fluctuations, magnetic fields and accelerated particles, respectively. Implications regarding the correlation functions of fluid quantities such as \mathbf{u} can be drawn in analogy to § 3.5.

In §4.1 below we study the scaling properties of the fluid equations of motion, under the simplifying assumptions of an ideal fluid and that corrections of order ϵ_B can be neglected. A closed set of equations is derived for the fluid component, and it is demonstrated that self-similar (scalable) solutions of the equations exist only for $s_u = s_B = 0$. In §4.2 we argue that under the assumption $R_{Lth} \ll L$, the fluid can be treated as infinitely conducting (as we show, the exact requirement is $R_{Lth}/L \ll \{v_s T/L, L/v_s T\}$).

One consequence of the scaling indices derived above is a divergence of the energy associated with the self-similar components. A flat power-law energy-spectrum of accelerated particles, $dn/dE \propto E^{-2}$ [Eq. (36) with $s_B = 0$], which is a natural consequence of the model and agrees with observations and with linear DSA theory, implies that the energy density diverges at large momenta. Similarly, a flat magnetic power-spectrum of the form $B_{ij}^{(2D)}(\mathbf{k}_\perp, L) \propto k_\perp^{-2}$ [Eq. (39) with $s_B = 0$] implies that the magnetic energy density diverges at large wavelengths (the same applies to the kinetic energy associated with the velocity fluctuations). Possible remedies for the divergence problem are outlined in § 4.3, but resolving the problem is beyond the scope of this paper.

4.1. Fluid equations

For simplicity, we focus below on relativistic shocks. We comment at the end of this subsection on the application of the analysis to non-relativistic shocks. As mentioned above, we consider the flow in the downstream frame.

The total electric current is $\mathbf{j} = \mathbf{j}_F + \mathbf{j}_h$. The fluid current may be written as

$$\mathbf{j}_F = \frac{c}{4\pi} \nabla \times \mathbf{B} - \mathbf{j}_h - \frac{1}{4\pi} \partial_t \mathbf{E}. \quad (44)$$

In order to guarantee conservation of charge we must include

$$\nabla \cdot \mathbf{E} = 4\pi(\rho_h + \rho_F) \quad (45)$$

as an independent equation, where ρ_h is the electric charge density carried by the accelerated component,

$$\rho_h = \sum_\alpha q_\alpha \int_{p > \xi_p e \bar{B} L/c} d^3 \mathbf{p} f_\alpha, \quad (46)$$

and ρ_F is the electric charge density carried by the fluid. Conservation of fluid energy and momentum is described by

$$\partial_\nu T_F^{\mu\nu} = F^{\mu\nu} j_{F\nu}, \quad (47)$$

where $T_F^{\mu\nu}$ is the fluid energy momentum tensor, $j_{F\nu}$ is the fluid four current, and $F^{\mu\nu}$ is the electromagnetic tensor. The fluid velocity \mathbf{u} is defined so that $T^{0i} = 0$ in a local frame moving with velocity \mathbf{u} . These equations can be closed with the addition of an "equation of state," relating the different components of $T^{\mu\nu}$ in the fluid rest frame.

As the energy density of the fluid must scale as L^0 , the above equations are consistent only with a scaling in which the EM fields and $T_F^{\mu\nu}$ both scale as L^0 , implying $s_u = s_B = 0$. However, since the equations may contain terms that can be neglected, and the scaling laws are likely to be relevant to fluctuations in $T^{\mu\nu}$ (imposed on a constant background) rather than to its average value, different scaling exponents may also be allowed. In order to examine this in more detail, we make the simplifying assumption of an ideal fluid, i.e. $T^{ij} \propto \delta^{ij}$ in the fluid rest frame. This is the case if the distribution of the fluid particles is approximately isotropic in the fluid's local rest frame, which is reasonable as their Larmor radius is much smaller than the length scale for variations in the magnetic field. Under this assumption, equation (47) can be written as

$$\partial_t [\gamma^2 (w_0 + w)] + \nabla \cdot [\gamma^2 (w_0 + w) \mathbf{u}] = \mathbf{E} \cdot \mathbf{j}_F + \partial_t P \quad (48)$$

and

$$\begin{aligned} \frac{\gamma^2 (w_0 + w)}{c^2} (\partial_t + \mathbf{u} \cdot \nabla) \mathbf{u} + \frac{\mathbf{E} \cdot \mathbf{j}_F + \partial_t P}{c^2} \mathbf{u} \\ = -\nabla P + \rho_F \mathbf{E} + \frac{1}{c} \mathbf{j}_F \times \mathbf{B}, \end{aligned} \quad (49)$$

where $P_0 + P$ and $w_0 + w$ are the pressure and rest frame enthalpy per unit volume, respectively, assumed to consist of a constant part, $P_0 \sim w_0 \sim \gamma_s^2 n_1 m_p c^2$, and a fluctuating part, P, w . Here, $\gamma \equiv (1 - u^2/c^2)^{-1/2}$ is the Lorentz factor associated with the fluid's velocity fluctuations. The fluid equations must be simplified by identifying terms that are negligible, in order to determine the correct scaling laws. As explained above, we assume that the magnetic force density, $c^{-1} |\mathbf{j}_F \times \mathbf{B}| \sim L^{-1} B^2 \sim L^{-1} \epsilon_B \gamma_s^2 n_1 m_p c^2$, makes a considerable contribution to the momentum balance [Eq. (49)]. This implies $P \lesssim \epsilon_B \gamma_s^2 n_1 m_p c^2 \sim \epsilon_B P_0$. We assume that $w/w_0 \sim P/P_0$, which holds for example for any equation of state where the

enthalpy is a function of the pressure alone, in particular this is true for a relativistic equation of state, $w_0 + w = 4(P_0 + P)$. We find $w \lesssim \epsilon_B \gamma_s^2 n_1 m_p c^2 \sim \epsilon_B w_0$. Comparing the first and the last terms in Eq. (49), combined with the above result, $L/T \sim u$, we find that $\gamma^2 u^2/c^2 \sim \epsilon_B$ and thus $\gamma \approx 1$ and the fluid fluctuations are non-relativistic. We thus find that the thermal energy P and the kinetic energy $U_u \sim w_0 u^2$ of the fluid fluctuations are related to the magnetic energy by $P, U_u \lesssim U_B$. Note that $\mathbf{E} \cdot \mathbf{j}_F \sim u B^2/L$ [since $E j_F \sim (u/cB)(cB/L)$]. Hence, equations (48) and (49) can be approximately written as

$$w_0 \nabla \cdot \mathbf{u} = 0 \quad (50)$$

and

$$\frac{w_0}{c^2} (\partial_t + \mathbf{u} \cdot \nabla) \mathbf{u} = -\nabla P + \rho_F \mathbf{E} + \frac{1}{c} \mathbf{j}_F \times \mathbf{B}. \quad (51)$$

In this case, we may eliminate the pressure from the equations by taking the curl of Eq. (51), yielding

$$\frac{w_0}{c^2} \{ \partial_t \nabla \times \mathbf{u} - \nabla \times [\mathbf{u} \times (\nabla \times \mathbf{u})] \} = \nabla \times (\rho_F \mathbf{E} + \frac{1}{c} \mathbf{j}_F \times \mathbf{B}). \quad (52)$$

Equations (3), (28)-(29), (41), (50) and (52), constitute a closed set of equations for the unknowns \mathbf{u}, f_α (for momentum $p > \xi_p e \bar{B} L/c$) and \mathbf{B} . As can be readily seen, these equations imply (and are consistent with) a scaling $s_B = s_u = 0$.

The above analysis is also applicable to non-relativistic shocks. A few comments should, however, be added. In the non-relativistic case, the electric field is much weaker than the magnetic field, $E \sim (u/c)B \ll (v_s/c)B \ll B$. In addition, it is expected that $T \sim L/u \ll L/c$. Thus, the terms $\partial_t f_\alpha$ (for relativistic momentum) and $q_\alpha \mathbf{E}$ in Vlasov's equation Eq. (28), and the term $c^{-1} \partial_t \mathbf{E}$ in Maxwell's equation $\nabla \times \mathbf{B} = 4\pi c^{-1} \mathbf{j} + c^{-1} \partial_t \mathbf{E}$, may be neglected. Since the particles of the thermal component are non-relativistic in this case, w_0/c^2 may be replaced in equations (50) and (52) by its non-relativistic limit, ρ_{Fm_0} (mass density). The assumption $w/w_0 \lesssim P/P_0$, which for non-relativistic particles reads $\rho_{Fm}/\rho_{Fm_0} \lesssim P/P_0$, is somewhat less justified but still reasonable. As mentioned above, these differences do not modify the scaling relations.

4.2. Infinite fluid conductivity

Here we argue that the assumption $R_{L,th} \ll L$ implies that the fluid can be treated as infinitely conducting (as we show below the exact requirement is $R_{L,th}/L \ll \{v_s T/L, L/v_s T\}$).

The fluid velocity is approximately equal to the the velocity of the proton component of the fluid. We now demonstrate that the electric and the magnetic forces acting on the proton component approximately cancel each other and thus lead to Eq. (41). Consider the proton fluid in a box of size $< L$ during a time scale $< T$, in which the magnetic and electric fields are approximately constant in space and time. The proton momentum inside the box is $\sim \gamma_s m_p n u L^3$. The time derivative of the momentum in the box originates from the electric force, $f_E \sim e n L T^3 \sim e n (L/cT) B L^3$, the magnetic force, $f_B \sim e n u / c B L^3$, and the flow of momentum into the box, $f_P \lesssim L^2 n (\gamma_s m_p v_s) v_s$. The ratio of the momentum flow to the electric force is of the order of

$$\frac{f_P}{f_E} \lesssim \frac{\gamma_s m_p v_s^2}{e B L} \frac{c T}{L} \sim \frac{R_{L,th}}{L} \frac{v_s T}{L} \ll 1. \quad (53)$$

Hence, the only force that can balance f_E is f_B . The forces are balanced only if $\mathbf{E} = -c^{-1} \mathbf{u} \times \mathbf{B}$. If the forces are not balanced, the proton fluid is accelerated. The time it takes the

velocity u to reach the scale L/T (for which $\mathbf{E} \sim -c^{-1} \mathbf{u} \times \mathbf{B}$), is very short, of the order of $\gamma_s m_p n (L/T) L^3 / e n L T^3 \sim (R_{L,th}/v_s T) T \ll T$. Therefore, we may assume that the forces are approximately balanced at any given time, and the fluid is nearly infinitely conducting.

4.3. Diverging Energy

As explained in the beginning of this section, the vanishing of the magnetic scaling index, s_B , implies logarithmic energy divergences. The divergence may be prevented if the scaling relations given in Eqs. (26) and (40) are approximate, rather than accurate. For example, high-order terms, $\propto 1/L, 1/L^2, \dots$, that were neglected in our analysis may introduce logarithmic corrections to the scaling relations. Alternatively, physical processes that were not included in the analysis, such as cooling, may limit the parameter range over which self-similarity is applicable, e.g. self-similarity may hold up to some cutoff momentum p_{max} or cutoff distance D_{max} .

Modeling GRB external shocks (Waxman 1995) and SNR shocks (Zhang 1993) implies that in both systems the maximal energy of accelerated ions is limited by the age (size) of the system, whereas the maximal energy of the accelerated electrons is limited by energy losses. If the accelerated electrons play an important role in the evolution, self-similarity may break-down at some scale associated with electron cooling. Otherwise, the accelerated proton configuration may remain self-similar beyond the electron-cooling scale. In this case, the accelerated protons have a time-dependent energy-cutoff and may (if their spectrum is sufficiently flat) modify the structure of the shock with time, rendering our assumption of a steady-state inaccurate (self-similarity may still exist). We are not aware of observational constraints (on the shock thickness, say) that rule out this possibility.

5. EXTENSIONS OF THE MODEL

In the previous sections we have motivated the self-similarity assumption based on observational evidence that is relevant directly to the downstream of strong, non-magnetized shocks. It is possible, however, that in other related circumstances, in which power-law distributions of energetic particles are interacting with non-magnetized MHD plasmas, similar scalable solutions arise. In § 5.1 we examine the possibility that the hydro-magnetic structure of the upstream is also self-similar. In § 5.2 we discuss time-dependent, homogenous toy models, in which energetic particles with a power-law distribution in momentum are added to a plasma.

5.1. Upstream

It is expected that the accelerated component precursor generates turbulence in the upstream (Blandford & Eichler 1987). In the context of GRB's, it was recently claimed that the magnetic field energy density in the upstream is larger than that typical to the typical ISM by at least 3 orders of magnitude (Li & Waxman 2006), which suggests that high energy particles generate waves upstream of the shock. If this is indeed the case, it is likely that higher momentum particles are important at larger distances from the shock, which suggests that the characteristic length scale for variations in the fields grows with the distance from the shock. Therefore, the EM structure in the upstream may also have a self-similar character, although we do not have as strong observational evidence for self-similarity in the upstream as we have for such behavior in the downstream.

Consider the conditions many skin depths upstream of the shock. The equations governing the accelerated component's distribution function and the EM fields are the same as for the downstream. In particular we expect the relation between the scaling indices to be

$$s_{p1} = s_{B1} + 1; \quad s_{f1} = -2s_{B1} - 4, \quad (54)$$

where the subscript 1 denotes the upstream. As explained in § 3.5, assuming that the accelerated component reaches the shock front, we expect the distribution function to have a power law momentum dependence with a power law index $l_p = s_f/s_p$. From the same considerations, we must have in the upstream $l_p = s_{f1}/s_{p1}$. We thus find that the scaling indices of the upstream and downstream are equal. In particular, for the expected value $s_B = 0$, the energy in the magnetic field does not decay as we go farther into the upstream. This result, which cannot be true for arbitrary distances in the upstream, is related to the diverging energy in accelerated particles. Note also, that the value of \bar{B} , which is constant according to our analysis in the upstream and far downstream regions, is expected to change considerably in the shock vicinity (distance of order l_{sd} where the self similarity breaks down), and thus is probably different in the upstream and downstream.

Although the scaling relations are the same for the upstream and the downstream, the accelerated distribution function can have a qualitatively different spatial dependence. Note that for sufficiently high momentum the distribution is continuous across the shock. In particular, for a given momentum, the accelerated particle distribution function in the upstream is expected to decay exponentially (if the acceleration process is DSA, see e.g. Kirk et al. 2000), while in the downstream it is expected to remain approximately constant.

The analysis of the fluid component in the upstream is more complicated, as the magnitude of the (velocity, pressure) fluctuations and the amount of fluid heating are unknown.

5.2. Homogenous configurations

In this subsection we consider the development of magnetic fields in homogenous configurations as a consequence of the interaction of the thermal fluid with the accelerated particles (for related simulations see, e.g., Lucek & Bell 2000; Bell 2004). Such configurations are much simpler to simulate and analyze than space-dependent configurations, and may give insights into dynamically important mechanisms.

If spatial inhomogeneity has an important role in the acceleration mechanism in collisionless shocks (as it does in the case of Fermi acceleration), it is likely that no acceleration takes place in homogenous configurations. In order to see the effects of an accelerated component on the dynamics, it would be interesting to perform homogenous simulations with an accelerated component (with a power-law distribution function) included in the initial conditions.

In the following, we assume a homogenous configuration with a relativistic accelerated component with some anisotropic distribution function $f_\alpha(\mathbf{p}) = g_\alpha(\mu)p^{l_p}$, $p > p_{min}$, included in the initial conditions, where $\mu = \cos(\mathbf{p} \cdot \hat{z})$ (the z axis is chosen to represent the direction of the shock normal; the cylindrical symmetry around this axis is present in planar non-magnetized shocks and there is no reason not to include it in homogenous simulations). We assume that the fluid component may be described by single fluid equations for which there is no inherent physical length scale. We assume initial neutrality, in the sense that any charge density (electric

current) implied by f_α is compensated by an opposite charge density (current) carried by the fluid.

Quite generally, a non-isotropic distribution is unstable. The distribution function is expected to evolve from the initial unstable configuration to a stable (probably isotropic) configuration by the development of instabilities followed by dissipation. Particles with larger momentum will respond more slowly to the generated EM fields (which are limited in strength by the initial energy) and on longer length scales (perhaps of the order of their Larmor radius). Fluctuations of the EM fields on small scales are expected to decay with time (Gruzinov 2001a) while EM field generation at later times due to instabilities in larger momentum regimes is expected to occur on longer length scales. It is thus likely that the magnetic field length scale grows with time. Self similarity is to be expected once the length scale of the magnetic field is much larger than the Larmor radius of particles having p_{min} .

The time development may be affected by the choice of g_α . In particular, the value of the bulk electric current carried by the initial population $\propto \int_{-1}^1 \mu [g_p(\mu) - g_e(\mu)]$ and bulk velocity $\propto \int_{-1}^1 \mu [g_p(\mu) + g_e(\mu)]$ may affect the nature of the instabilities involved. As we show in this subsection, the self similarity assumption (as long as it is valid) allows determination of some physically interesting quantities without dependence on the precise instability mechanism.

In this case, we cannot assume a steady-state. However, there is a full (three dimensional) translational symmetry (homogeneity). We consider averaged quantities at fixed times. In particular, Eq. (15) and Eq. (16) are replaced by:

$$\langle f_\alpha \rangle(\mathbf{p}, t) \equiv \lim_{r \rightarrow \infty} \frac{1}{\frac{4}{3}\pi r^3} \int_{x' < r} d^3 \mathbf{x}' f_\alpha(\mathbf{x} + \mathbf{x}', \mathbf{p}, t) \quad (55)$$

and

$$B_{ij}(\Delta \mathbf{x}, \Delta t, t) \equiv \lim_{r \rightarrow \infty} \frac{1}{\frac{4}{3}\pi r^3} \int_{x' < r} d^3 \mathbf{x}' B_i(\mathbf{x} + \mathbf{x}', t) B_j(\mathbf{x} + \Delta \mathbf{x} + \mathbf{x}', t + \Delta t), \quad (56)$$

where these functions do not depend on \mathbf{x} due to the homogeneity (\bar{B} defined similarly).

We assume that a scaling property, following Eqs. (23)-(25), is obtained at late times, i.e.

$$\bar{B}(L) = \left(\frac{L}{L_0} \right)^{s_B} \bar{B}(L_0), \quad (57)$$

$$\langle f_\alpha \rangle(\mathbf{p}, L) = \left(\frac{L}{L_0} \right)^{s_f} \langle f_\alpha \rangle \left[\frac{\mathbf{p}}{(L/L_0)^{s_p}}, L_0 \right], \quad (58)$$

and

$$B_{ij}(\Delta \mathbf{x}, \Delta t, L) = \left(\frac{L}{L_0} \right)^{2s_B} B_{ij} \left[\frac{\Delta \mathbf{x}}{L/L_0}, \frac{\Delta t}{(L/L_0)^{s_t}}, L_0 \right], \quad (59)$$

with $L \propto t^{1/s_t}$, $T \propto t$ ($s_t > 0$).

An important difference with respect to the shock case arises from the absence of a finite bulk velocity, and therefore the assumption that time scales as distance no longer applies in general. We study cases in which the magnetic fields are stronger than electric fields and thus restrict $s_t \geq 1$. A value of $s_t > 1$ is consistent with Vlasov's equation, Eq. (28), if we neglect the time derivative term and the electric field term, which is justified for $s_t > 1$.

The distribution function of the accelerated component is by definition finite at $t \rightarrow 0$ (also at $L \rightarrow 0$). In analogy to Eq. (34), we therefore have $\langle f_\alpha \rangle(\mathbf{p}, t) \propto p^{s_f/s_p}$ for $p \rightarrow \infty$. On the other hand, $\langle f_\alpha \rangle(\mathbf{p}, t=0) \propto p^{l_p}$, which implies that $s_f/s_p = l_p$ (this also shows that a finite initial distribution must be a power-law in order to achieve self-similarity). From Vlasov's equation (and the expression for the electric current) we find, as for the shock case, that

$$s_p = s_B + 1, \quad s_f = -2s_B - 4. \quad (60)$$

Here it is useful to solve for the scaling indices in terms of the initial power-law index l_p ,

$$s_B = -\frac{l_p+4}{l_p+2}, \quad s_p = -\frac{2}{l_p+2}, \quad s_f = -\frac{2l_p}{l_p+2}. \quad (61)$$

Assuming that the fluid can be considered as infinitely conducting (see § 4.2), we have $u \sim L/T$ so $s_u = 1 - s_t$. Assuming further that the magnetic force is not negligible in the fluid momentum equation (51) we find $s_u = s_B$ (this is reasonable as the energy source is the energetic component, and energy is transferred to the fluid through the magnetic fields). Together with Eq. (61) we have

$$s_t = 1 - s_B = \frac{2(l_p+3)}{l_p+2}. \quad (62)$$

In particular this implies $\bar{B} \propto L^{s_B} \propto t^{s_B/s_t} = t^{-(l_p+4)/2(l_p+3)}$.

6. SOME GENERAL IMPLICATIONS

If self-similarity holds, it has important implications for any model of particle acceleration and/or field generation. In § 6.1 we show that a previously suggested model, that describes the flow in terms of merging current filaments (Medvedev et al. 2005) in a self similar manner, must be generalized in order to be a self-consistent model. We show that after the appropriate generalization the model follows the scaling relations derived in § 5.2, and that the generalization significantly modifies the model's predictions. In § 6.2 we discuss the relevance of our analysis to DSA.

6.1. Current merger model

Medvedev et al. (2005) suggest a model of coalescing electric current filaments in a quasi two-dimensional configuration for describing the magnetic field evolution in the downstream of collisionless shocks. In this model there is no distinction between accelerated and thermal particles, so it does not hold information regarding the energy dependence of the particle distribution function. As the model is essentially homogenous and self-similar, it is interesting to compare it to the scalings derived in § 5.2.

This model assumes that electromagnetic instabilities in the shock lead to the formation of current filaments, which may be approximated as infinite in length and having equal electric currents oriented parallel to the flow, half of the currents positive (oriented along the flow) and half negative. The filaments are assumed to be distributed randomly in space. This simple model assumes that current filament coalescence evolves in discrete steps. In each step the filaments carrying similarly oriented currents, are divided into neighboring pairs, which attract each other and merge. Two filaments with diameter D , inertial mass per unit length μ , and current I , unite to form a new filament of diameter $D' = \sqrt{2}D$ (conserving area), mass per unit length $\mu' = 2\mu$, and current $I' = 2I$. In each step, the

typical distance d between neighbor filaments with similarly oriented currents, grows by a factor of $\sqrt{2}$, $d' = \sqrt{2}d$, as a consequence of the reduced filament number density. It is assumed that $d \simeq 2D$ which implies that the filaments roughly fill the space with their area. Initially, all the filaments are identical (except for the sign of the current), and are hence identical at any given time. The coalescence time, here denoted by τ_{coa} , is estimated by analyzing two isolated, parallel, infinite current filaments attracting each other.

The fact that D and d change in each merger by the same factor, implies that the configuration following each merger is identical to that before the merger, with re-scaled parameters. In particular, the filament coalescence time, $\tau_{coa} \propto \mu^{1/2} c D/I$, and the maximal velocity during coalescence, $v \propto I/(c\mu^{1/2})$, scale as $\tau'_{coa} = \tau_{coa}$ and $v' = \sqrt{2}v$. The fact that the filament velocity grows with time, led the authors to the conclusion, that velocities of the order of the speed of light will be reached. Once the filaments move with $v \sim c$, the coalescence temporal behavior changes considerably.

This suggested merger model is problematic, as it implies that the magnetic field grows by a factor of $\sqrt{2}$ in each step. For example, the magnetic field produced by a single filament at its edge, $B = 4I/cD$, scales as $B' = \sqrt{2}B$. More generally, the coalescence suggested is self-similar with $\mathbf{j}'(\mathbf{x}) = \mathbf{j}(\mathbf{x}/\sqrt{2})$, implying $\mathbf{B}'(\mathbf{x}) = \sqrt{2}\mathbf{B}(\mathbf{x}/\sqrt{2})$. To see this, note that the current density carried by each filament, $j \sim I/D^2$, does not change in the coalescence, while the filament diameter and distance between filaments grow by $\sqrt{2}$. The fact that the magnetic field grows by a constant factor in each step, implies that after a few steps the magnetic energy density grows beyond equipartition, which is impossible. This can be corrected by changing appropriately the coalescence conditions.

Since the physical process of the merger is complicated, there is no simple way to determine the post-merger current directly. In general, one should therefore set the current of the merged filament to $(\sqrt{2})^\zeta I$ where ζ is a parameter of the model (the mass per unit length is set to 2μ since mass is conserved). In this case, the coalescence is self-similar with $\mathbf{j}'(\mathbf{x}) = (\sqrt{2})^{\zeta-2}\mathbf{j}(\mathbf{x}/\sqrt{2})$, implying that $\mathbf{B}'(\mathbf{x}) = (\sqrt{2})^{\zeta-1}\mathbf{B}(\mathbf{x}/\sqrt{2})$ and the magnetic field amplitude does not grow for $\zeta \leq 1$. The scaling of the filament coalescence time and maximal velocity changes to $\tau'_{coa} = (\sqrt{2})^{2-\zeta}\tau_{coa}$ and $v' = (\sqrt{2})^{\zeta-1}v$.

The (necessary) generalization of the current merger model strongly influences the conclusions that can be drawn based on this model. The growth in length scale is only determined up to a free parameter ζ . In order for the magnetic field not to diverge with time, we must have $\zeta \leq 1$ (if the magnetic field amplitude is postulated to be constant in time, $\zeta = 1$). This implies that the velocities do not grow (remain constant for $\zeta = 1$) and therefore do not reach the speed of light.

The (corrected) scalings are compatible with the scalings for the fluid derived in § 5.2, with $s_B = \zeta - 1$, $s_t = 2 - \zeta$, $s_u = \zeta - 1$. Note, that the self-similar analysis allows us to reach most of the physically interesting conclusions without making oversimplifying and model-specific assumptions, such as the calculation of the length of the time step using two isolated filaments in the current merger model.

It has been claimed (Milosavljević & Nakar 2005a) that current filaments are unstable to kink-like modes and that the two dimensional configuration is therefore disrupted. We

note that even if the instability is efficient, this does not rule out the model. Since the instabilities are derived within the framework of MHD, for which the above scalings hold, the perturbation's growth rate scales as all other time scales, i.e. $\tau'_{ins} = (\sqrt{2})^{2-\zeta} \tau_{ins}$ where τ_{ins} is the inverse growth rate. If initially $\tau_{ins} > \tau_{coa}$ (which is not ruled out), the filaments merge before they are destroyed by the instabilities, and this holds, i.e. $\tau_{ins} > \tau_{coa}$, for all subsequent mergers.

6.2. Diffusive shock acceleration

Diffusive shock acceleration (DSA) is the mechanism believed to be responsible for the production of non-thermal populations of charged particles in collisionless shocks. In this first-order Fermi acceleration process, particles gain energy by repeatedly bouncing between the converging upstream and downstream flows. In the lack of a self-consistent theory for the interaction between electromagnetic waves and accelerated particles in collisionless shocks, most progress was made under the "test-particle" approximation. In this approach, the effects of the waves are modelled by some particle-scattering Ansatz, while the influence of the particles on the waves and on the shock structure are neglected (for reviews, see Drury 1983; Blandford & Eichler 1987; Malkov & Drury 2001).

In the case of non-relativistic shocks, DSA has been successful in reproducing the power-law spectra observed in strong shocks, under very general assumptions regarding the scattering mechanism (Krymskii 1977; Axford et al. 1977; Bell 1978; Blandford & Ostriker 1978). The analysis of relativistic shocks is more complicated, mainly because the non-thermal particle distribution is not isotropic. The particle spectrum was calculated in relativistic shocks under various assumptions regarding the scattering mechanism, using monte-carlo simulations [e.g. Ellison et al. (1990); Ostrowski (1991)], and by numerical (Kirk & Schneider 1987; Gallant & Achterberg 1999; Vietri 2003; Blasi & Vietri 2005) or analytical (Keshet & Waxman 2005) study of the transport equations. In general, a power-law distribution function of accelerated particles is found, with indices that depend on details of the model and usually satisfy $l_p < -4$. In the case of ultra-relativistic shocks with isotropic, small-angle scattering, numerical studies have converged on a spectral index $l_p \simeq -4.22$ (Bednarz & Ostrowski 1998; Kirk et al. 2000; Achterberg et al. 2001), in agreement with GRB afterglow observations and with the analytic result $l_p = 38/9$ (Keshet & Waxman 2005). However, this value was demonstrated numerically (Ballard & Heavens 1992; Ostrowski 1993; Ellison & Double 2002, 2004; Meli & Quenby 2003b,a; Bednarz 2004; Niemiec & Ostrowski 2004; Lemoine & Pelletier 2003; Lemoine & Revenu 2006) and analytically (Keshet & Waxman 2005) to be sensitive to the scattering mechanism, which is poorly constrained.

In our analysis, the fluctuations in the fluid provide a natural scattering mechanism for the accelerated particles. Since the analysis reflects near equipartition between fluid fluctuations, accelerated particles and magnetic fields, it does not naturally evoke (but does not rule out) a test-particle approach. A spectral index $l_p \neq 4$ can be reconciled with our analysis only if we relax some of our assumptions. For example, if we assume that the magnetic field energy is constant with distance from the shock, $l_p < -4$ would imply that the currents carried by the accelerated component \mathbf{j}_h decrease faster than the total current $\mathbf{j} \sim \nabla \times \mathbf{B}$, and thus the effect of the accelerated particles on the magnetic field is negligible at large distances

(in this case, the test particle assumption is self-consistent). If, on the other hand, we assume that the magnetic field decreases with distance as $s_B = -(l_p + 4)/(l_p + 2)$ (see § 3.5), a value $l_p < -4$ would contradict our assumptions regarding the self similarity of the fluid component (for example, the magnetic force would become negligible in the momentum conservation equation, or the fluid would no longer be highly conductive and its currents would become negligible).

The assumption of self-similarity places constraints on some properties of DSA. As an illustration, consider the case of small-angle scattering, parameterized by a propagation-angle diffusion coefficient $D_{\mu\mu}$. The stationary transport equation can be written as (Kirk & Schneider 1987):

$$\gamma_i(v_i/c + \mu_i) \partial_{z_s} \langle f_i \rangle(p_i, \mu_i, z) = \partial_{\mu_i} [D_{\mu\mu}(\mu_i, p_i, z) \partial_{\mu_i} \langle f_i \rangle] \quad (63)$$

where subscript $i = 1, 2$ denotes upstream or downstream parameters, respectively, $\gamma_i = (1 - v_i^2/c^2)^{-1/2}$, and $\mu = \cos(\mathbf{p}_i \cdot \hat{\mathbf{z}})$. The momentum \mathbf{p}_i (and therefore also μ) is measured in the fluid rest frame, whereas z is measured in the shock frame. With boundary conditions $\langle f_i \rangle(p_i, \mu_i, -\infty) = 0$, $\langle f_i \rangle(p_i, \mu_i, \infty) = \langle f_i \rangle_\infty(p_i)$ and $\langle f_1 \rangle(p_1, \mu_1, 0) = \langle f_2 \rangle(p_2, \mu_2, 0)$, where (p_1, μ_1) and (p_2, μ_2) are related through an appropriate Lorenz boost. The solution is unique up to the normalization of $\langle f_i \rangle$ (Kirk et al. 2000).

The small-angle scattering assumption requires that the Larmor radius of the particles R_L is much larger than the magnetic field length-scale L . In our framework, for any given momentum p this is true up to a limited distance from the shock (where $L < pc/eB$). Consistency of DSA theory thus requires that $\langle f_i \rangle(p_i, \mu_i, z)$ converge to its limiting value $\langle f_i \rangle_\infty(p_i)$ within this range.

In order to comply with the self similar scaling of Eq. (24), we must require that

$$\langle f_i \rangle(p_i, \mu_i, z) = \left(\frac{z}{z_0} \right)^{s_f} \langle f_i \rangle \left[\frac{p_i}{(z/z_0)^{s_p}}, \mu_i, z_0 \right]. \quad (64)$$

This scaling can be reconciled with the transport equation [Eq. (63)] if and only if the diffusion function scales as

$$D_{\mu\mu}(p_i, \mu_i, z) = \frac{z_0}{z} D_{\mu\mu} \left[\frac{p_i}{(z/z_0)^{s_p}}, \mu_i, z_0 \right]. \quad (65)$$

The boundary conditions are invariant to the above scaling (at the shock front $p_1 \propto p_2$). Under this scaling, $\langle f_i \rangle(p_i, \mu_i, z) \propto p_i^{l_p}$ at $z = \pm\infty$, where $l_p = s_f/s_p$. The values of s_f and l_p are determined in a non-trivial way by the function $D_{\mu\mu}(p_i, \mu_i, z)$. If $s_p = 1$, as is expected when the plasma is highly conductive, we may write Eq. (65) as

$$D_{\mu\mu}(p_i, \mu_i, z) = z^{-1} \tilde{D}_{\mu\mu}(\mu_i, p_i/z). \quad (66)$$

As an example of the above scaling, consider a highly relativistic particle scattered by weak magnetic fluctuations of correlation length $L \ll R_L$. The particle trajectory may then be described as a random walk in μ , and the resulting diffusion function is $D_{\mu\mu}(p, \mu, z) = D(\mu)LR_L^{-2}$. For $L \propto z$ (and $s_B = 0$), we obtain $D_{\mu\mu}(p, \mu, z) \propto z^{-1}(p/z)^{-2}$.

7. DISCUSSION

We have studied the consequences of the assumption that the downstream flow of non-magnetized, collisionless shocks is self-similar. This assumption is motivated by the existence of a strong magnetic field many skin depths downstream of the

shock front, as inferred from observations of GRB afterglows and young SNR's. This suggests that the correlation length of magnetic field fluctuations, L , diverges with the distance D from the shock front. Although our analysis was motivated by evidence for self-similarity in GRB afterglows, and possibly also in SNRs, it may apply to other systems with similar characteristics, such as the shocks involved in the large scale structure of the Universe.

As the electromagnetic fields and particle distributions at any given point fluctuate with time, a stationary shock structure may be described by the averages (over planes parallel to the shock front) and correlation functions of the fluctuating quantities, which depend only on the distance from the shock (see § 2.3). The self-similarity assumption implies that $L \propto D$ and that the averages and correlation functions at different distances D from the shock, corresponding to different values of L , are related to each other by simple scaling transformations (see § 3.2), e.g.

$$\bar{B}(L) = \left(\frac{L}{L_0}\right)^{s_B} \bar{B}(L_0),$$

$$\langle f_\alpha \rangle(\mathbf{p}, L) = \left(\frac{L}{L_0}\right)^{s_f} \langle f_\alpha \rangle \left[\frac{\mathbf{p}}{(L/L_0)^{s_p}}, L_0 \right],$$

$$B_{ij}(\Delta \mathbf{x}, \Delta t, L) = \left(\frac{L}{L_0}\right)^{2s_B} B_{ij} \left[\frac{\Delta \mathbf{x}}{L/L_0}, \frac{\Delta t}{(L/L_0)^{s_t}}, L_0 \right],$$

where the scaling exponent of the magnetic field must satisfy

$$-1 < s_B \leq 0.$$

A schematic illustration of a self similar downstream configuration is presented in figure 1.

We have argued (see § 3.3) that the similarity assumption suggests that the plasma may be approximately described as a combination of two self-similar components: a kinetic component of energetic particles, and an MHD-like component representing "thermal" particles. We have argued that the energetic particles are likely to carry a significant fraction of the current, and derived (using the Maxwell-Vlasov equations) the scaling of the characteristic time for variations in the physical quantities, the scaling of the characteristic particle momentum and the scaling of the particle distribution function normalization:

$$s_t = 1, \quad s_p = s_B + 1, \quad s_f = -4 - 2s_B.$$

These relations imply that the characteristic Larmor radius of energetic particles scales as L , and that the energy density of energetic particles in any momentum interval, with the interval scaling as L^{s_p} , scales as the magnetic field energy density $\propto L^{2s_B}$. We have then shown (see § 3.5) that (under the assumption that accelerated particles reach the shock front and/or are advected to the downstream) the spectrum of accelerated particles is

$$dn/dE \propto E^{-2/(s_B+1)},$$

and that the scaling of the magnetic correlation function (for $\Delta x \rightarrow \infty$) is

$$\langle B_i(\mathbf{x})B_j(\mathbf{x} + \Delta \mathbf{x}) \rangle \propto \Delta \mathbf{x}^{2s_B}.$$

Similar conclusions can be drawn regarding various other correlation functions.

The "thermal" particles were discussed in § 4. In § 4.2 we have argued that the thermal component may be considered

as an infinitely conducting fluid. We have shown that in this case $s_B = 0$ and the scalings are completely determined, e.g. $dn/dE \propto E^{-2}$ and $B \propto D^0$, with possible logarithmic corrections. We have derived in § 4.1 a closed set of equations for the fluid component, under the simplifying assumptions of an ideal fluid and neglecting corrections of order ε_B .

The self similarity assumption and its implications do not hold for arbitrarily large distances and high particle momenta where new physical processes that were not taken into account in our analysis come in to play. For example, our assumption of an infinite planar shock is invalid at distance scales of the order of the blast wave radius, and the use of the Vlasov equation is invalid for high momenta where radiative effects cannot be ignored. Upper cutoffs to the distance scale and the momentum range described by the self-similar solution, or logarithmic corrections to this solution, are possible remedies of the energy divergence when $s_B = 0$, as discussed in § 4.3.

If self-similarity holds, it has important implications for any model of particle acceleration and/or field generation. In § 6.2 we have shown that the velocity-angle diffusion coefficient for small-angle scattering in diffusive shock acceleration models must satisfy $D_{\mu\mu}(\mathbf{p}, D) = D^{-1} \tilde{D}_{\mu\mu}(\mathbf{p}/D)$ (where \mathbf{p} is the particle momentum).

In § 6.1 we have discussed the model suggested by Medvedev et al. (2005) for the generation of a large scale magnetic field through hierarchical merger of current-filaments. We have shown that in order to avoid a diverging magnetic field, the model must be generalized by allowing a more general scaling of the electric current of merged filaments. The generalized model follows the scaling laws we have derived in § 5.2. This implies that the self-similar analysis allows us to reach most of the physically interesting conclusions without making oversimplifying and model-specific assumptions (such as those related to the calculation of the merger time). The predictions of the generalized model differ substantially from those of the original model. It predicts, e.g., a scale independent merging velocity, rather than an increasing velocity approaching the speed of light (this is valid for a non-decaying magnetic field; for a decaying field, the velocity decreases with scale). Finally, we have shown that the instability of current filaments (which was pointed out by Milosavljevic & Nakar 2005a) does not necessarily imply that the current merger model is not viable.

In § 5.2 we have pointed out that the self-similarity assumptions may be tested through their predictions for the evolution of homogenous (time-dependent) plasmas, which may be accessible to direct numerical simulations. An inclusion (at the initial conditions) of an anisotropic, power-law spectrum of high energy particles, $dn/dE \propto E^{2+l_p}$, in homogenous simulations may lead to a self-similar evolution in time, described by the scaling exponents given in Eq. (61). Assuming that the fluid can be considered as infinitely conductive, we predict that the magnetic field evolution follows $B \propto t^{-(l_p+4)/2(l_p+3)}$.

Our self-similar model predicts the scaling of all physical quantities related to the accelerated particles, electromagnetic fields and fluid fluctuations. In particular, the particle spectrum is related to the magnetic field scaling: An accelerated particle distribution with a spectral index $l_p < -4$ indicates a decay of the magnetic field amplitude with distance from the shock according to $D^{-(l_p+4)/(l_p+2)}$. Such a decay of the magnetic field may be detectable, for example through the spatial dependence of synchrotron emission from non-thermal electrons gyrating in the downstream magnetic fields.

Finally, we should emphasize two major open questions related to our analysis, which need to be resolved. First, the validity of the description of the "thermal" component in terms of single-fluid MHD equations requires verification. Second, the diverging energy in accelerated particles that results from the distribution $n(E) \propto E^{-2}$, indicates that our assumptions cannot be valid for arbitrarily high momentum (see discussion and possible remedies at the end of § 3.5). A similar

divergence is identified in the energy of magnetic fields and fluid fluctuations.

This work was supported in part by ISF and AEC grants. We thank A. Gruzinov, A. Loeb & A. Sagiv for helpful discussions.

APPENDIX

COLLISIONLESS SHOCKS IN 3D PARTICLE-IN-CELL SIMULATIONS

In recent years, particle in cell (PIC) simulations have provided important preliminary clues to the nature of collisionless shocks. Fully three-dimensional PIC simulations have began to explore aspects of such shocks in non-homogeneous (Nishikawa et al. 2003; Frederiksen et al. 2004; Spitkovsky 2005) and homogeneous (Silva et al. 2003; Jaroschek et al. 2004; Romanov et al. 2004) flows. The main conclusions relevant for collisionless shocks are:

- Confirmation that shocks in pair-plasma (with no highly accelerated particles) are mediated by electromagnetic, two-stream (Weibel-like) instabilities if the upstream is sufficiently non-magnetized (magnetic energy less than $\sim 1\%$ of the kinetic energy; Spitkovsky 2005) and cold. In interpenetrating shells, this instability produces filaments in density (if $\Gamma \gtrsim 5$) and in electric current (Jaroschek et al. 2005), initially with \lesssim skin depth thickness, and transverse (perpendicular to the flow) magnetic fields. Electrons in ion-electron plasma behave similarly (Frederiksen et al. 2004).
- Preliminary evidence for the existence of relativistic, collisionless shocks in a non-magnetized pair-plasma. Spitkovsky (2005) resolves a shock-like behavior in a 3D simulation of interpenetrating pair-plasma shells, each with Lorentz factor $\Gamma = 15$. A density jump in approximate agreement with the Rankine-Hugoniot adiabat extends over $\sim 70l_{sd}$, and coincides with a region of near-equipartition magnetic fields. Here, $l_{sd} = c/\omega_p$ and $\omega_p = (4\pi ne^2/\Gamma m)^{1/2}$ are the skin-depth and plasma frequency, respectively, of simulated particles of mass m , number density n and Lorentz factor Γ .
- Possible indications for self-similarity. In interpenetrating plasma shells, the filaments merge after saturation and grow in a hierarchical process, maintaining a configuration of similar features on gradually larger scales, with magnetic fields decaying slowly and possibly saturating at $\epsilon_B \lesssim 1\%$ [in pair plasmas; Silva et al. (2003); Medvedev et al. (2005)]. Frederiksen et al. (2004; Figure 3) provide evidence that the power-spectrum of transverse magnetic fields is roughly a power-law, $P_k \propto k^{-\alpha}$ with $\alpha \simeq 2.3 - 3.0$, extending to gradually larger scales.

Present 3D PIC simulations are limited to small simulation-box volumes, $V < 10^6 l_{sd}^3$, and to short simulation durations, $T < 10^3 \omega_p^{-1}$. Here, ω_p and l_{sd} corresponds to the species with fastest-response; simulating an ion-electron plasma implies much smaller volumes and durations when written in terms of the ion parameters. In order to resolve any effects associated with the ions, an effective, small proton to electron mass ratio, $\tilde{m}_p/m_e \lesssim 20$ (with present computational resources) must be used, and the preliminary results thus obtained are not easily extrapolated to more realistic mass ratios. These constraints limit the relevance of any conclusion drawn from such simulations, and may even undermine their reliability:

- The length of the simulation box parallel to the flow is too small in most cases to resolve a shock, even in pair-plasma [with the possible exception of Spitkovsky 2005]. The configuration found in most simulations thus represents merely a transient stage in the formation of a shock, which may bare little relevance to its steady-state. Moreover, the short length of the box suppresses longitudinal modes of long wavelengths, thus distorting the plasma evolution by effectively reducing it to 2D. For example, an exponential decay of the magnetic energy (after growth saturation) abruptly stops in simulations (Silva et al. 2003; Jaroschek et al. 2005), possibly due to this effect.
- The small size of the simulation box (\lesssim tens of skin-depths) perpendicular to the flow places an artificial cutoff on transverse modes with long wavelengths. Simulations indicate that the transverse scale of the most energetic modes grows rapidly, reaching the box size cutoff at early stages of the simulation (Silva et al. 2003, Figure 3; Frederiksen et al. 2004, Figures 3-4). After this occurs, the simulations are strongly affected by the boundary conditions, and the simulated evolution is probably highly distorted.
- The Larmor radius of particles of Lorentz factor γ is $R_L = l_{sd}[\epsilon_B(\gamma^2 - 1)/2\Gamma(\Gamma - 1)]^{-1/2}$, where Γ is the average Lorentz factor. A simulation box tens of skin-depths long is therefor not sufficiently large to simulate particle magnetization when the ratio between magnetic and thermal energy densities is $\epsilon_B \lesssim 1\%$. Moreover, the box is much too small to resolve acceleration of particles to high energies, so any Fermi-like acceleration process is suppressed. Electrons are observed to be accelerated in ion-electron simulations (Nishikawa et al. 2003; Hededal et al. 2004), but to energies smaller than $\Gamma m_p c^2$.

REFERENCES

Achterberg, A., Gallant, Y. A., Kirk, J. G., & Guthmann, A. W. 2001, MNRAS, 328, 393

Axford, W. I., Leer, E. & Skadron, G. 1977, Proc. 15th Int. Cosmic Ray Conf., Plovdiv (Budapest: Central Research Institute for Physics), 11, 132

Ballard, K. R. & Heavens, A. F. 1992, MNRAS, 259, 89

Bamba, A., Yamazaki, R., Ueno, M., & Koyama, K. 2003, ApJ, 589, 827

Bednarz, J. 2004, PASJ, 56, 923

Bednarz, J. & Ostrowski, M. 1998, Physical Review Letters, 80, 3911

Begelman, M. C., Rees, M. J., & Sikora, M. 1994, ApJ, 429, L57 (1994); Bell, A. R. 1978, MNRAS, 182, 147

Bell, A. R. 2004, MNRAS, 353, 550

Bell, A. R. 2005, MNRAS, 358, 181

Berger, E., Kulkarni, S. R., & Frail, D. A. 2003, ApJ, 590, 379

Blandford, R. D. & Ostriker, J. 1978, ApJ, 221, L29

Blandford, R. & Eichler, D. 1987, Phys. Rep., 154, 1

Blandford, R. D. & McKee, C. F. 1976, Phys. Fluids, 19, 1130

Blasi, P. & Vietri, M. 2005, ApJ, 626, 877

Dieckmann, M. E., Shukla, P. K., & Drury, L. O. C. 2006, MNRAS, 367, 1072

Drury, L. O. 1983, Reports of Progress in Physics, 46, 973

Drury, L. O'C., Markiewicz, W. J., & Völk, H. J. 1989, A&A, 225, 179

Eichler, D. & Waxman, E. 2005, ApJ, 627, 861

Ellison, D. C. & Double, G. P. 2002, Astroparticle Physics, 18, 213

—. 2004, Astroparticle Physics, 22, 323

Ellison, D. C., Reynolds, S. P., & Jones, F. C. 1990, ApJ, 360, 702

Frail, D. A., Waxman, E., & Kulkarni, S. R. 2000, ApJ, 537, 191

D. A. Frail et al. 2001, ApJ, 562, L55

Frederiksen, J. T., Hedenfeld, C. B., Haugbølle, T., & Nordlund, Å. 2004, ApJ, 608, L13

Freedman, D. L., & Waxman, E. 2001, ApJ, 547, 922

Gallant, Y. A. & Achterberg, A. 1999, MNRAS, 305, L6

Gruzinov, A. 2000, arXiv:astro-ph/0012364

Gruzinov, A. 2001a, ApJ, 563, L15

—. 2001b, arXiv:astro-ph/0111321

Gruzinov, A. & Waxman, E. 1999, ApJ, 511, 852

Heddel, C. B., Haugbølle, T., Frederiksen, J. T. & Nordlund, Å. 2004, ApJ, 617, L107

Jaroschek, C. H., Lesch, H., & Treumann, R. A. 2004, ApJ, 616, 1065

—. 2005, ApJ, 618, 822

Kadanoff, L. P., et al. 1967, Reviews of Modern Physics, 39, 395

Kato, T. N. 2005, Phys. Plasmas 12, 080705

Keshet, U., Waxman, E., & Loeb, A. 2004, ApJ, 617, 281

Keshet, U. & Waxman, E. 2005, Physical Review Letters, 94, 111102

Kirk, J. G., Guthmann, A. W., Gallant, Y. A., & Achterberg, A. 2000, ApJ, 542, 235

Kirk, J. G. & Schneider, P. 1987, ApJ, 315, 425

Krall, N. A. 1997, Advances in Space Research, 20, 715

Krymskii, G. F. 1977, Dokl. Akad. Nauk SSSR, 234, 1306

Lemoine, M. & Pelletier, G. 2003, ApJ, 589, L73

Lemoine, M. & Revenu, B. 2006, MNRAS, 366, 635

Lucek, S. G., & Bell, A. R. 2000, MNRAS, 314, 65

Li, Z. & Waxman, E. 2006, arXiv:astro-ph/0603427

Loeb, A. & Waxman, E. 2000, Nature, 405, 156

Lyubarsky, Y. & Eichler, D. 2005, arXiv:astro-ph/0512579

Malkov, M. A. & Drury, L. O'C. 2001, Rep. Prog. Phys. 64 429

Maraschi, L. 2003, in AGNs: from Central Engine to Host Galaxy, Eds. S. Collin, F. Combes & I. Shlosman. ASP Conference Series, **290** 275 (2003)

Medvedev, M. V., Fiore, M., Fonseca, R. A., Silva, L. O., & Mori, W. B. 2005, ApJ, 618, L75

Medvedev, M. V. & Loeb, A. 1999, ApJ, 526, 697

Meli, A. & Quenby, J. J. 2003a, Astroparticle Physics

—. 2003b, Astroparticle Physics

Milosavljevic, M. & Nakar, E. 2005a, arXiv:astro-ph/0508464

—. 2005b, arXiv:astro-ph/0512548

Niemiec, J. & Ostrowski, M. 2004, ApJ, 610, 851

Nishikawa, K.-I., Hardee, P., Richardson, G., Preece, R., Sol, H., & Fishman, G. J. 2003, ApJ, 595, 555

Ostrowski, M. 1991, MNRAS, 249, 551

—. 1993, MNRAS, 264, 248

Panaiteescu, A. & Kumar, P. 2002, ApJ, 571, 779

Peacock, J. A. 1981, MNRAS, 196, 135

Piran, T. 2005, AIP Conf. Proc., 784, 164, arXiv:astro-ph/0503060

Romanov, D. V., Bychenkov, V. Y., Rozmus, W., Capjack, C. E., & Fedosejevs, R. 2004, Physical Review Letters, 93, 215004

Silva, L. O., Fonseca, R. A., Tonge, J. W., Dawson, J. M., Mori, W. B., & Medvedev, M. V. 2003, ApJ, 596, L121

Spitkovsky, A. 2005, AIP Conf. Proc., 801, 345, arXiv:astro-ph/0603211

Vietri, M. 2003, ApJ, 591, 954

Vink, J. & Laming, J. M. 2003, ApJ, 584, 758

Völk, H. J., Berezhko, E. G., & Ksenofontov, L. T. 2005, A&A, 433, 229

Wallace, J. M. & Epperlein, E. M. 1991, Phys. Fluids B, 3, 1579

Wang, X., Loeb, A., & Waxman, E. 2002, ApJ, 568, 830

Waxman, E., & Shvarts, D. 1993, Physics of Fluids A, 5, 1035

Waxman, E. 1995, Phys. Rev. Lett., 75, 386

Waxman, E. 1997, ApJ, 485, L5

Wiersma, J. & Achterberg, A. 2004, A&A, 428, 365

Zeldovich, Ya. B. & Raizer, Yu. P. 1968, Physics of Shock Waves and High-Temperature Hydrodynamic Phenomena, Chapter XII (New York: Academic).

Zhang, M. 1993, Proc. 23th ICRC (Calgary) 2, 374

Zhang, B. & Mészáros, P. 2004, International Journal of Modern Physics A, 19, 2385